Making Ferromagnetic Metal MnSi Ultrathin film Ferromagnetic Semiconductor

Zhao-hua Cheng (成昭华）

State Key Laboratory of Magnetism, Institute of Physics, Chinese Academy of Sciences, Beijing 100080, P.R. China

(中国科学院物理研究所磁学国家重点实验室）

研究方向和内容

基础、应用基础

- 自旋电子学
- 磁性纳米结构
- 新型稀土磁性材料
- 磁性氧化物
- 特种磁性材料及其应用
- 分子磁性
- 中子散射
- 超精细相互作用
- 实验技术（磁性测量、设备研制）
- 磁性理论

组织结构

中国科学院

中国科学院物理所

实验室室务委员会

磁学国家重点实验室

实验室学术委员会

办公室

研究体系

技术体系

赵同云

王芳卫

研究组M01

韩秀峰

研究组M02

孙继荣

研究组M03

成昭华

研究组M04

吴光恒

研究组M05

磁性纳米结构与磁共振

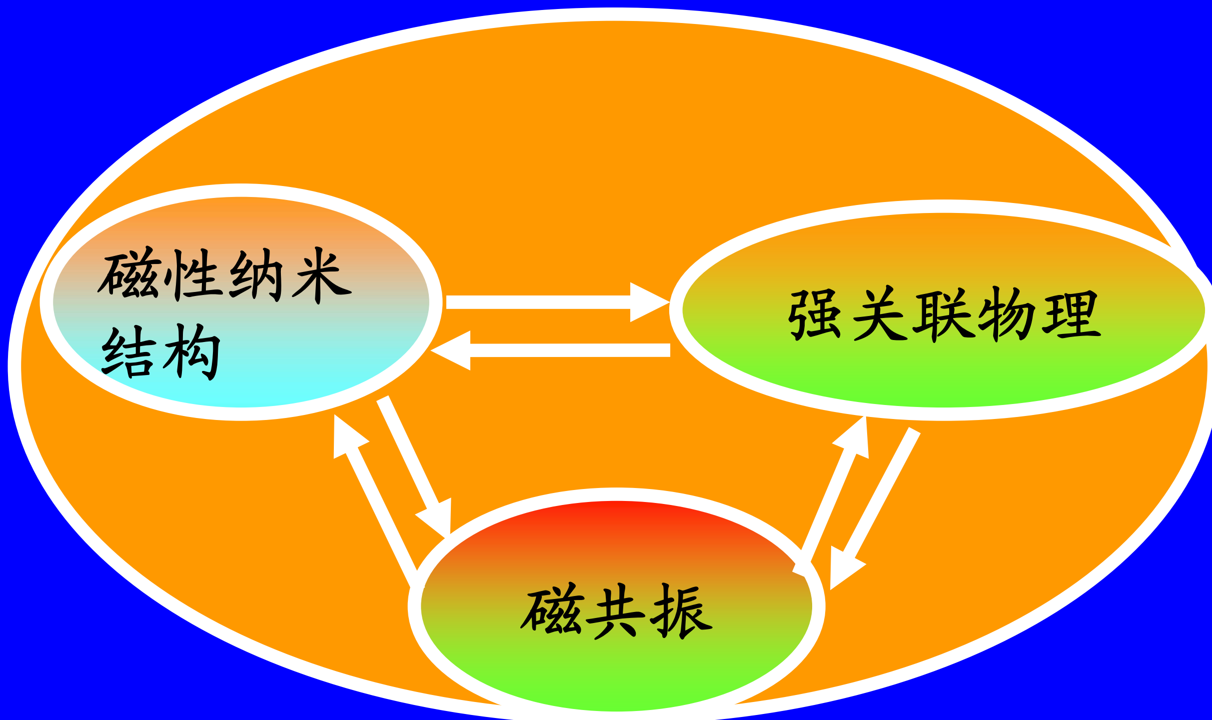

孙　阳
张向群
成昭华

杨海涛

博士生　12-15人

磁性纳米结构与磁共振

单晶生长炉(2002)

电化学实验室（**2003)**

MBE/SPM/SMOKE/MS(2004)

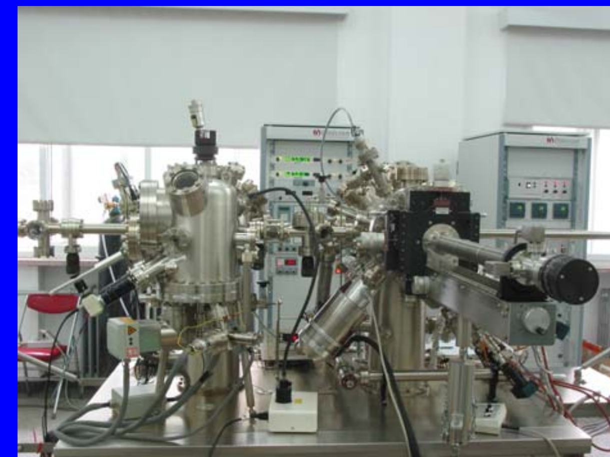

多电极磁输运（**2002)**

穆斯堡尔谱仪(2003)

电子自旋共振**(2006)**

磁性纳米结构与磁共振

磁学国家重点实验室
公共磁性测量和结构分析平台

物理所微加工

XRD

MFM

SQUID

PPMS

0-7T
4-400K

0-14T
0.3-400K

Outline

- Motivation
- Preferential arrangement and Controllable Growth of Mn Nanodots
- Fabrication of MnSi ultrathin film on Si(111)
- Magnetic and Magnetotransport Properties of MnSi Film on Si(111)
- Thickness-driven MIT Transition
- Summary

特征物理长度

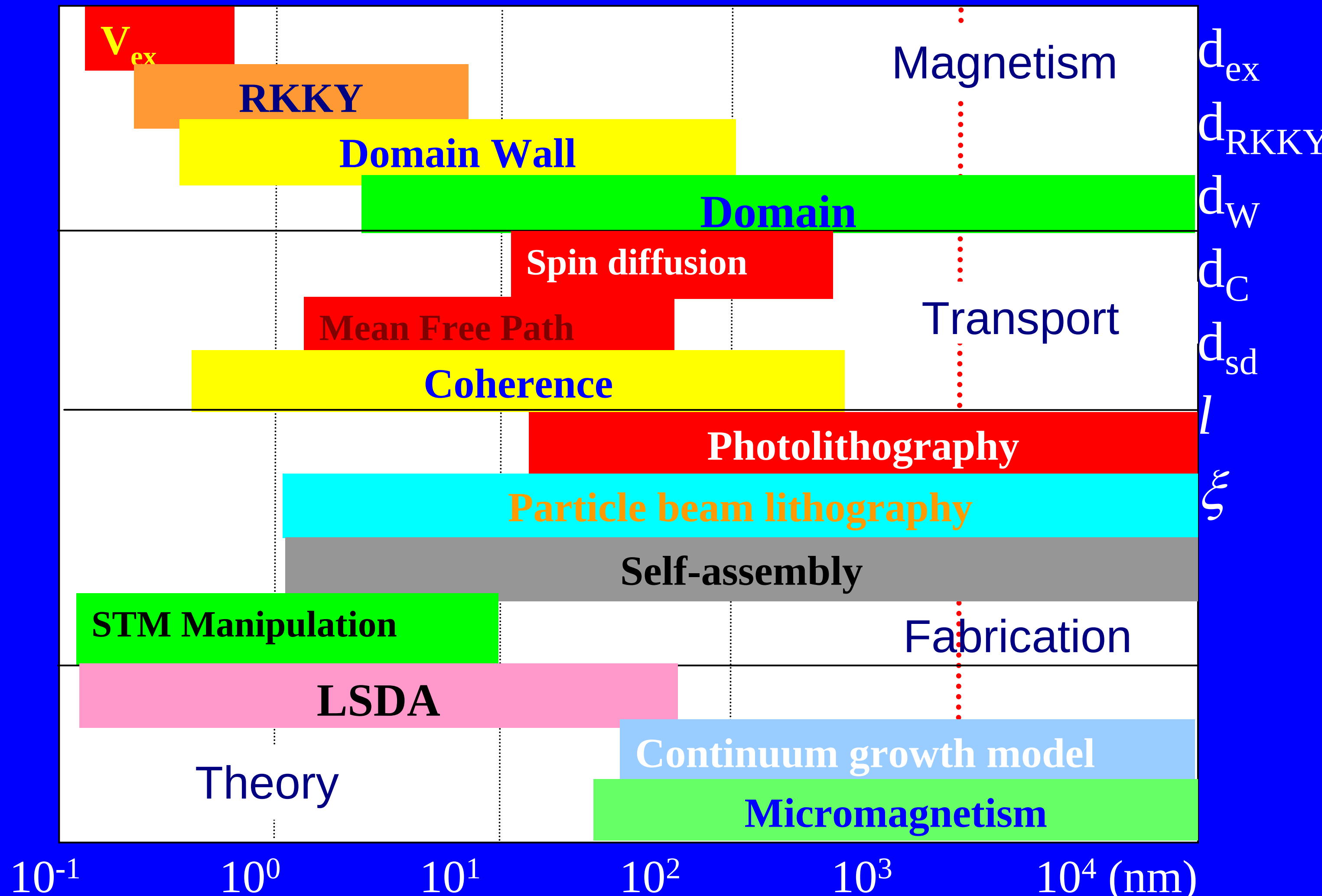

V_{ex}
RKKY
Domain Wall
Domain
Magnetism
Spin diffusion
Mean Free Path
Coherence
Transport
Photolithography
Particle beam lithography
Self-assembly
STM Manipulation
Fabrication
LSDA
Continuum growth model
Micromagnetism
Theory
d_{ex}
d_{RKKY}
d_W
d_C
d_{sd}
l
ξ
10^{-1} 10^{0} 10^{1} 10^{2} 10^{3} 10^{4} (nm)

Anomalous Magnetism in Small Mn Clusters

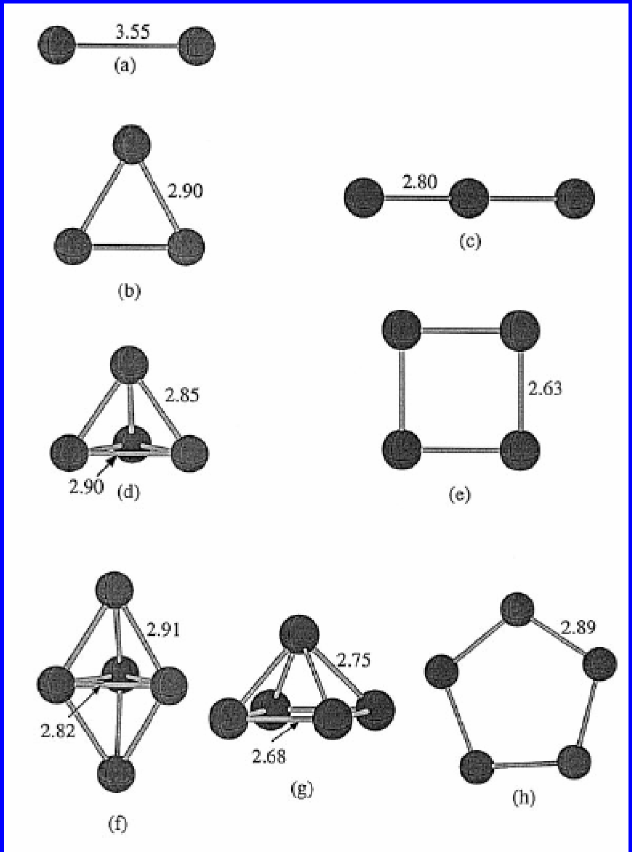

MRAM

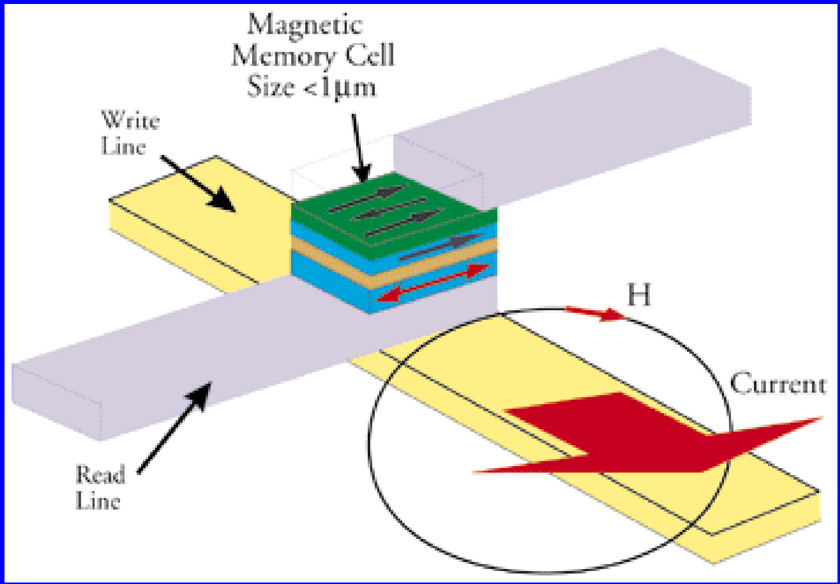

SFET

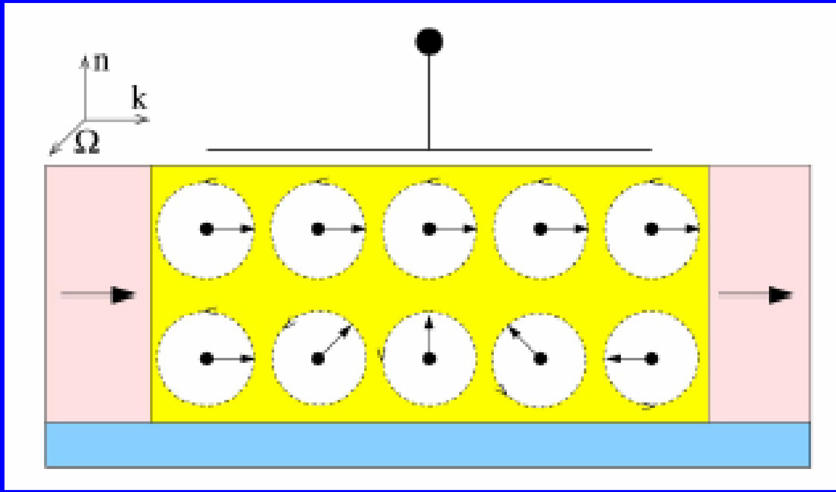

Fundamental Obstacles for Spin-injection

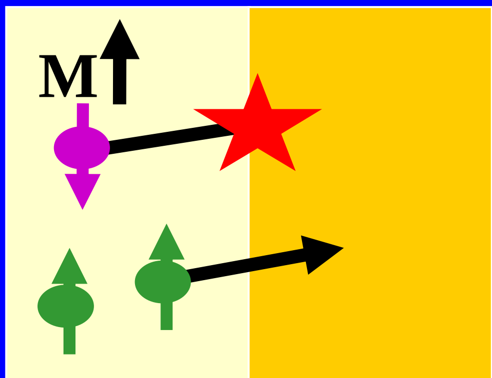

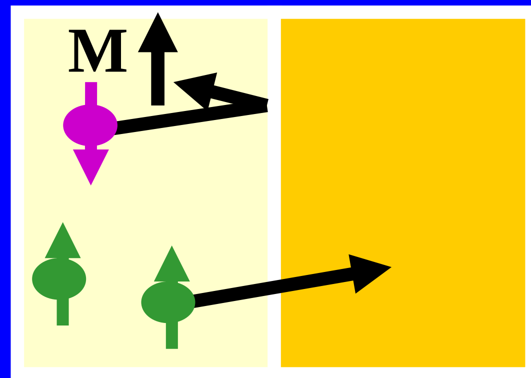

- Lattice mismatch
- Conductivity mismatch

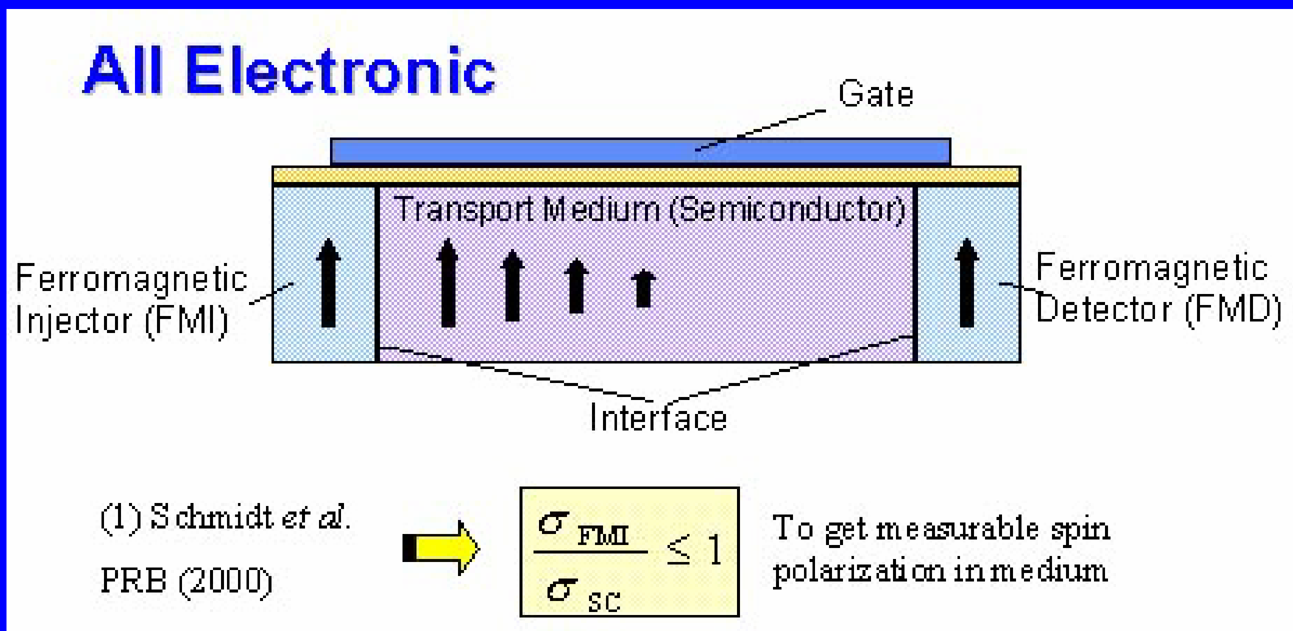

Epitaxial Growth of metal or metal Silicides on Si

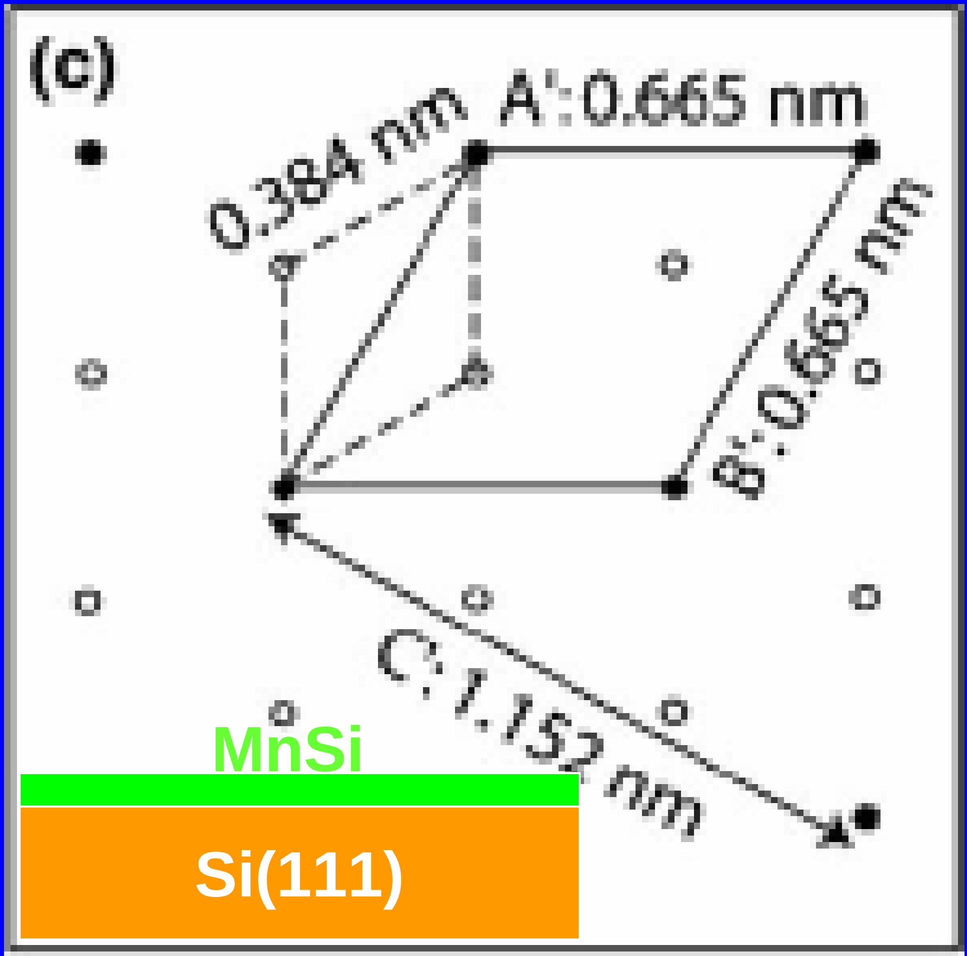

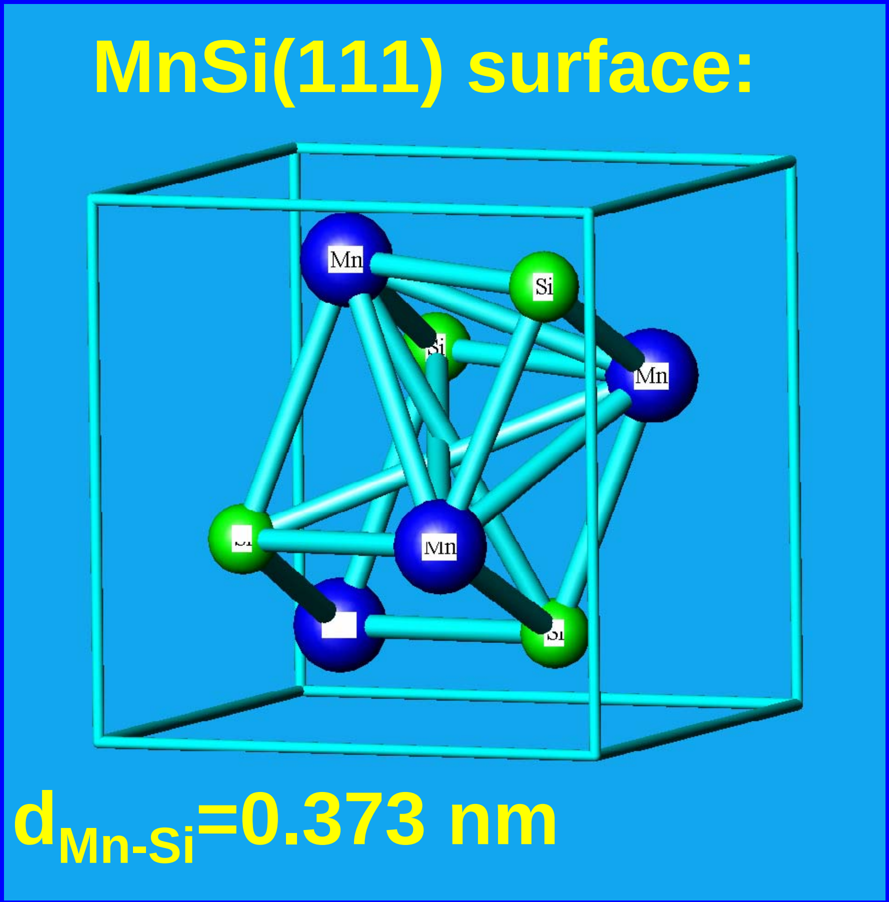

MnSi(111) surface:A=B=0.645nm,C=1.17nm

Ferromagnetic and Metallic Properties of MnSi bulk intermetallic Compounds

FeSi, CoSi, NiSi   weak, or non-magnetic

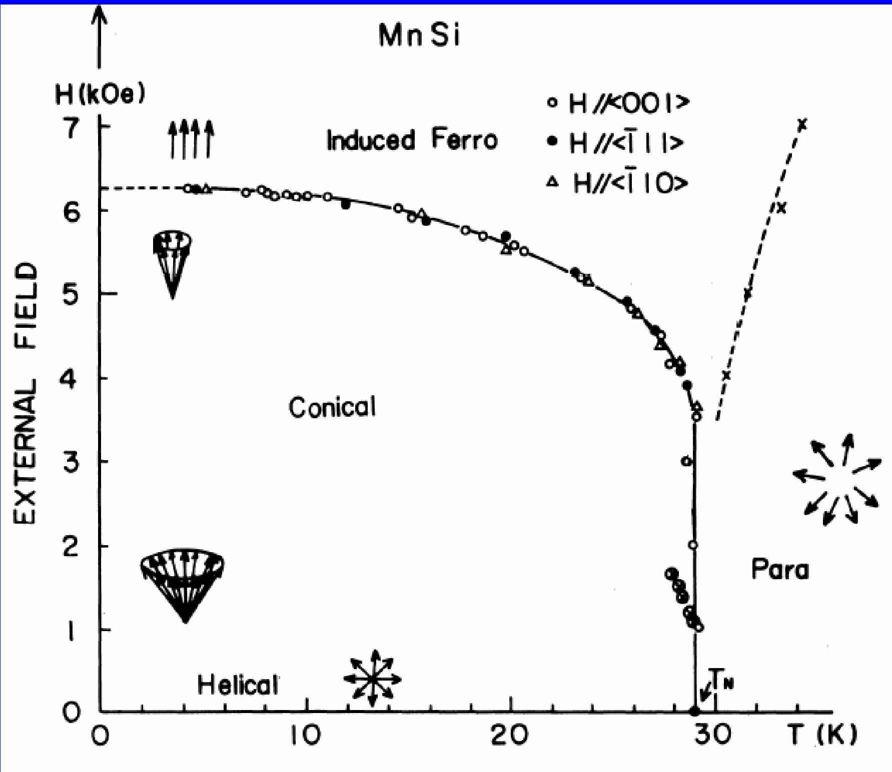

FIG. 1. Magnetic phase diagram of MnSi.

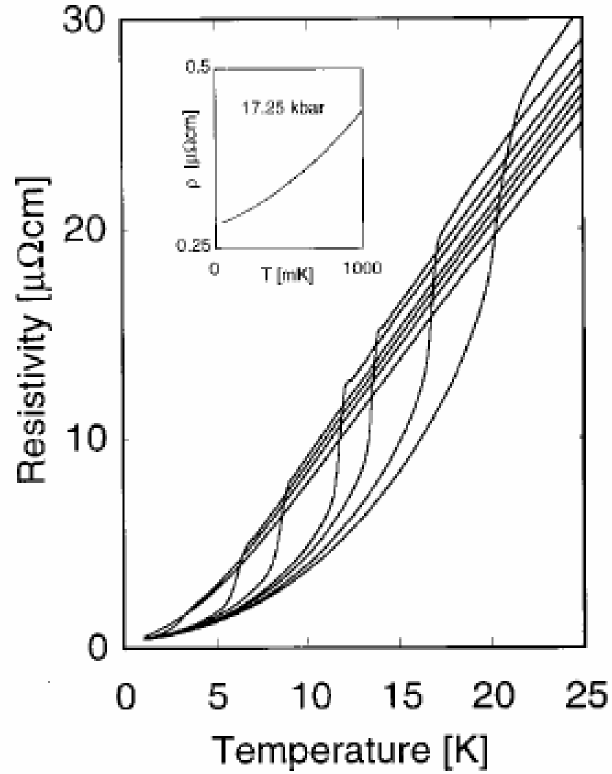

C. Pfleider, PRB,55,8330(1997)

Scaling Theory of Localization

$$g = G/(e^2/\hbar)$$

$$\beta(g) = \frac{d\ln g}{d\ln L} = \frac{L}{g}\frac{dg}{dL}$$

$\beta(g) = 1$ Ohm's-law

$\beta(g) > 0$ Extended state

$\beta(g) < 0$ Localized state

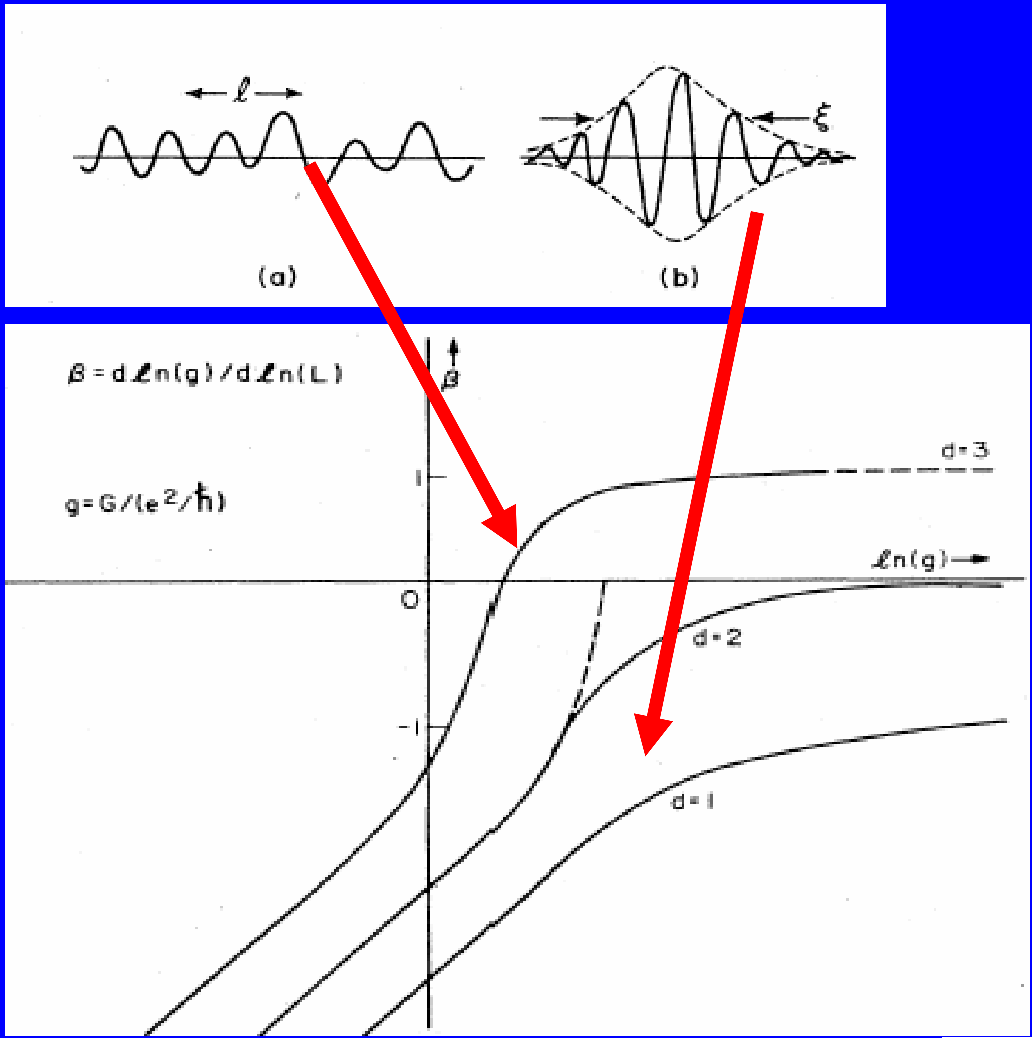

D.J. Thouless, PRL,39,1167(1977)
P.W. Anderson, PRL,43,718(1979)

Experimental Studies of Localization

Cu on glass 11.9nm

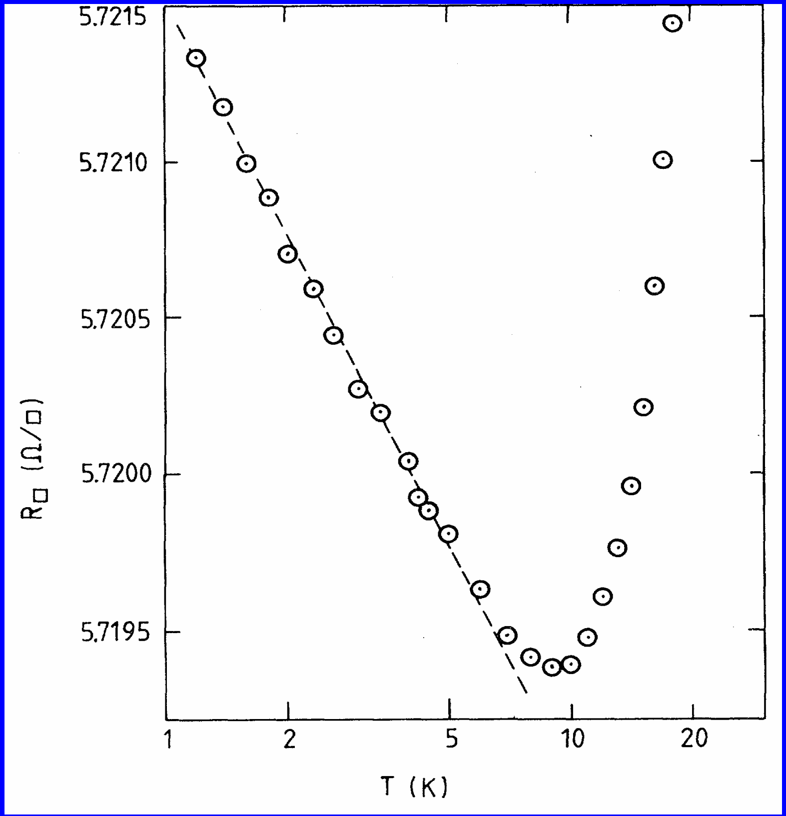

L. Van de dries, PRL 46, 565(1981)

Ag/Si(111)-7×7

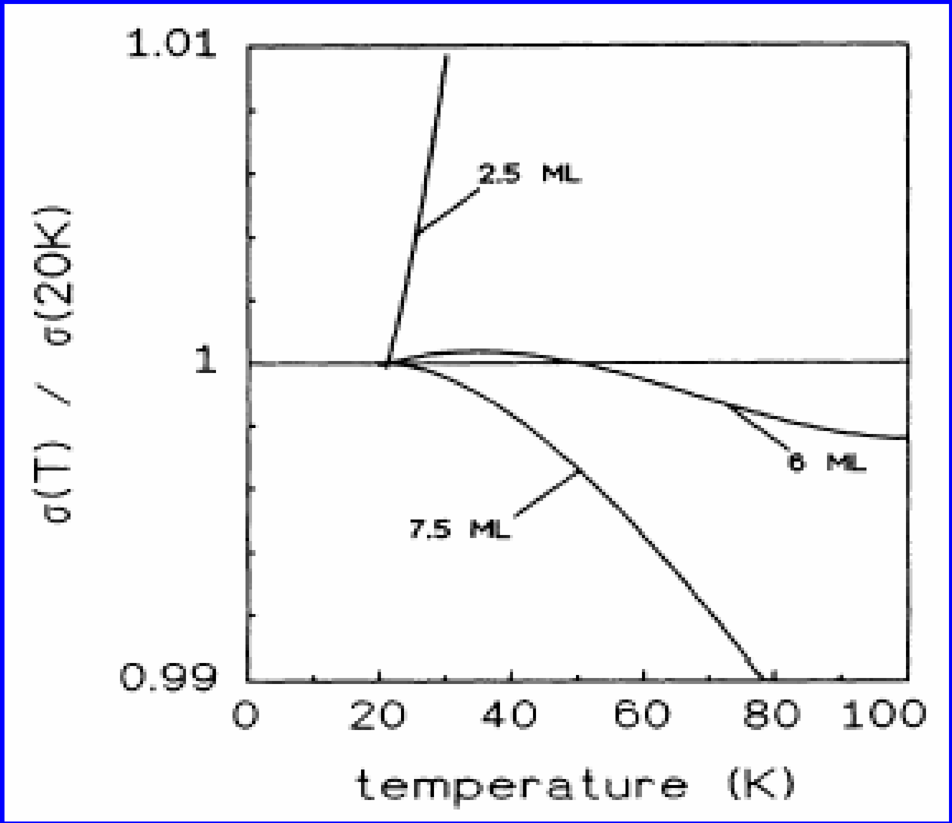

PRB 45 11430

II. Preferential arrangement and Controllable Growth of Mn Nanodots

LED/AES

Mössbauer Spectrometer

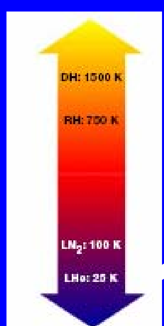

VT-SPM

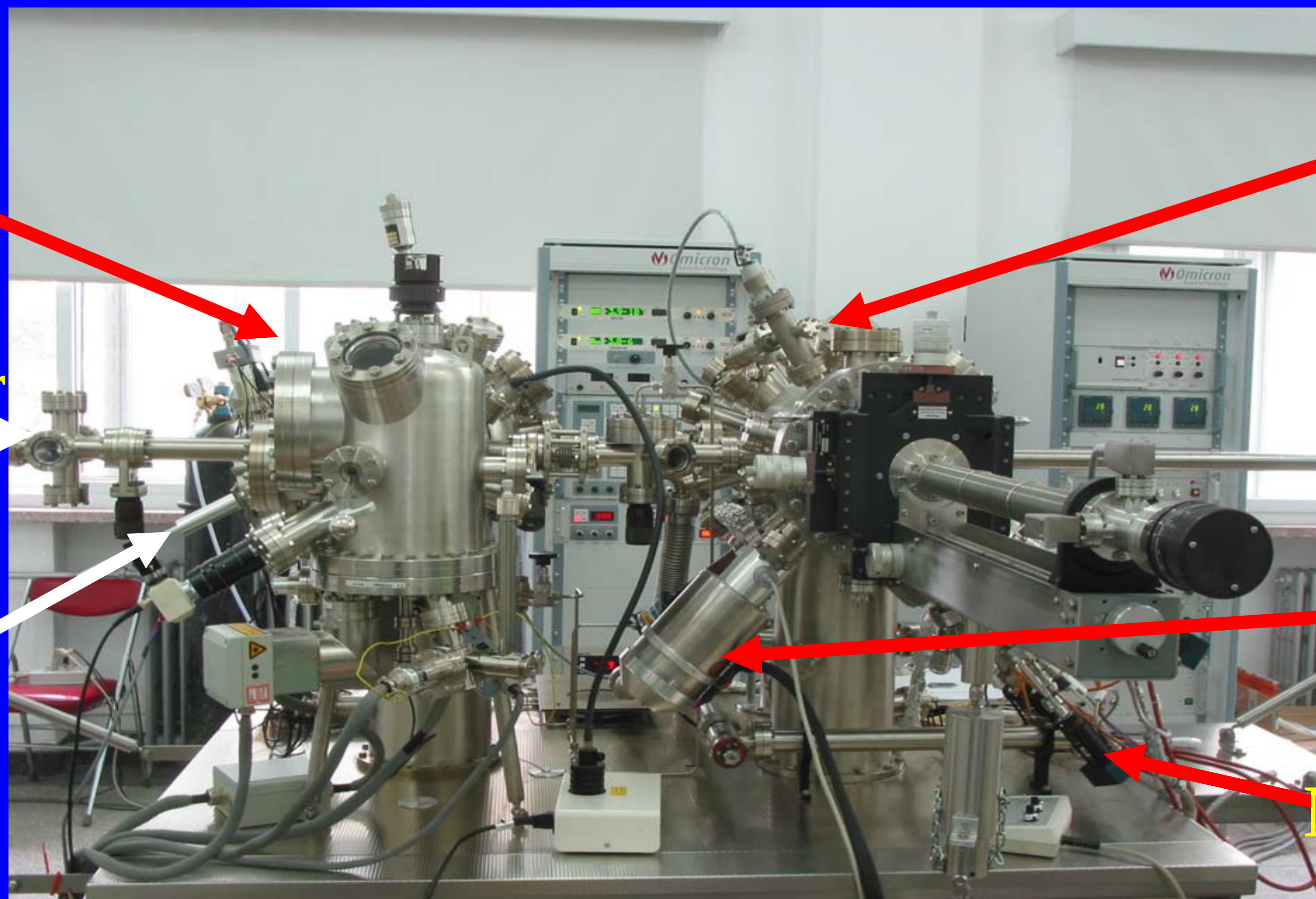

MOKE

RHEED

MBE/EB

Well-defined size of Si(111)-7×7 reconstructed surface

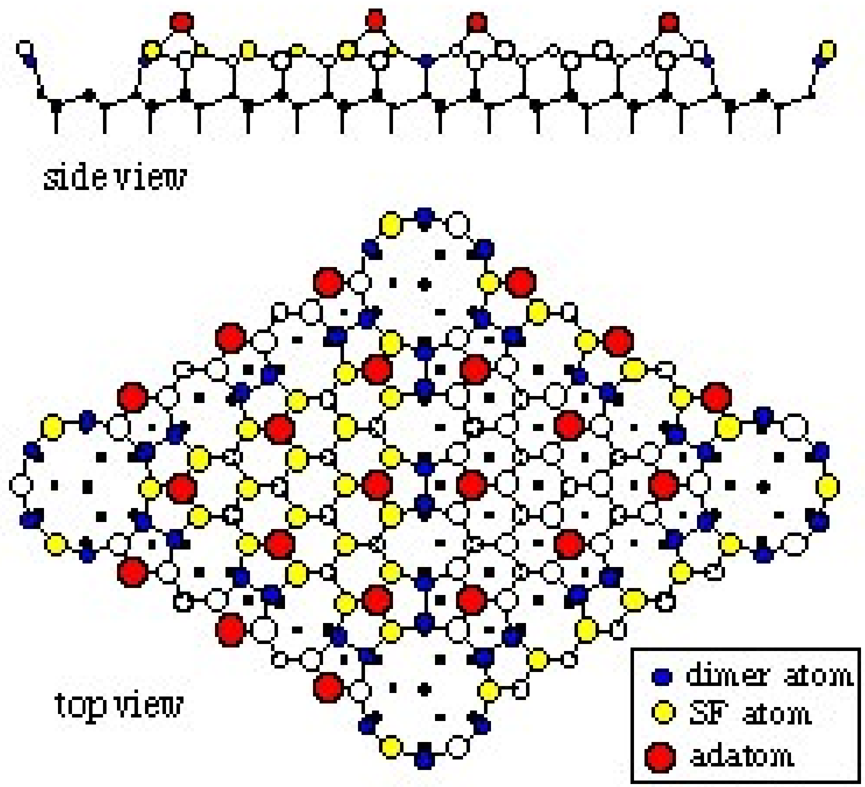

Unit cell of Si(111)-7x7 DAS structure

dI/dV mapping

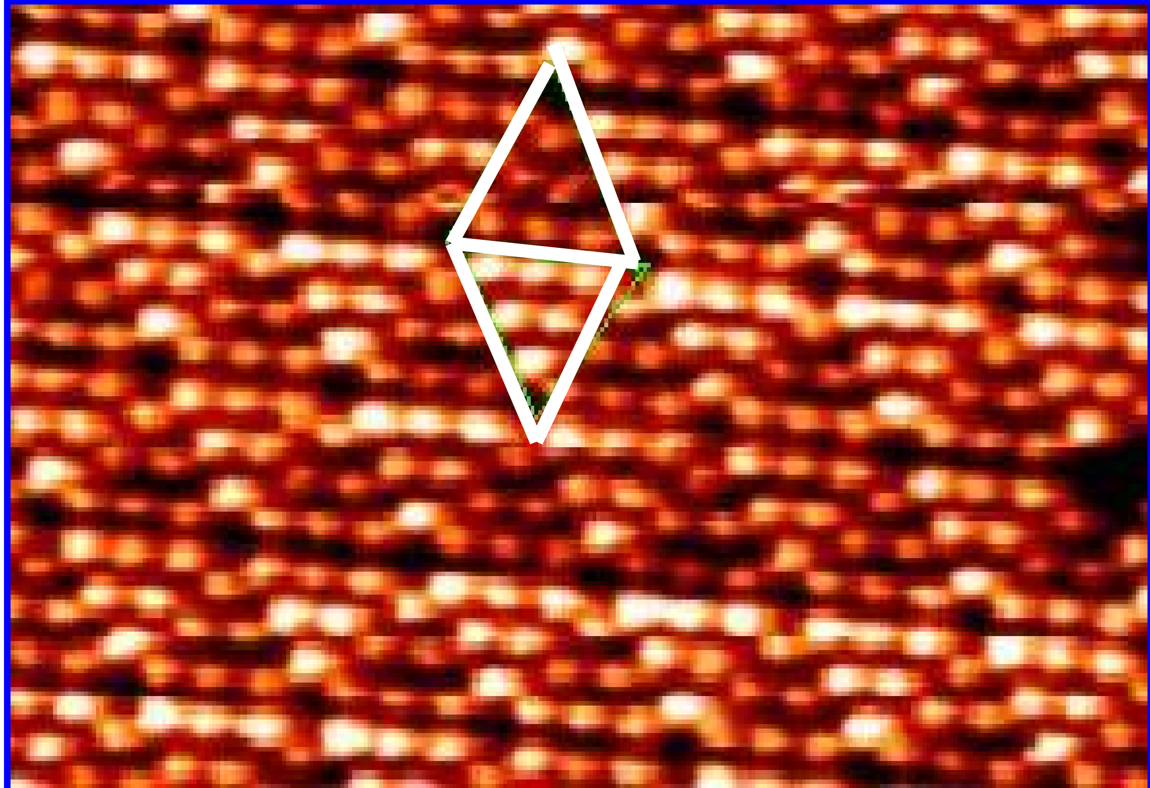

K. Takayanagi et al., Surface Sci. 164(1985),367

II. Preferential arrangement and Controllable Growth of Mn Nanodots

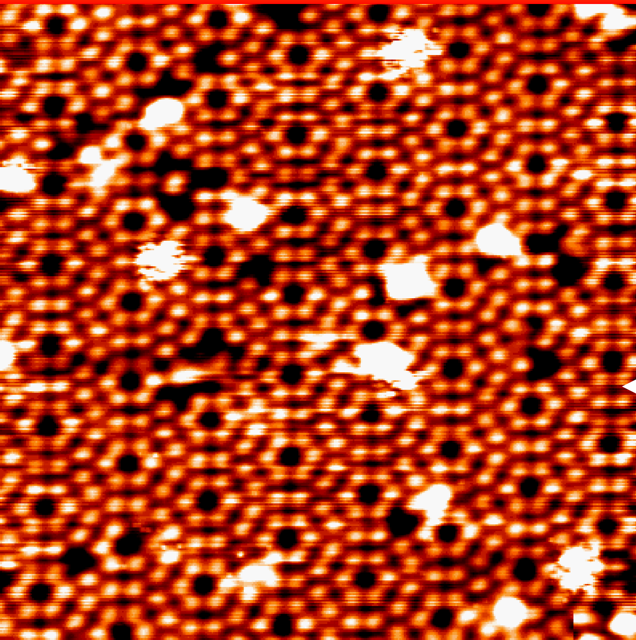

Room-temperature Growth

Complex the deposition and diffusion process

0.02 ML
20×20nm^2

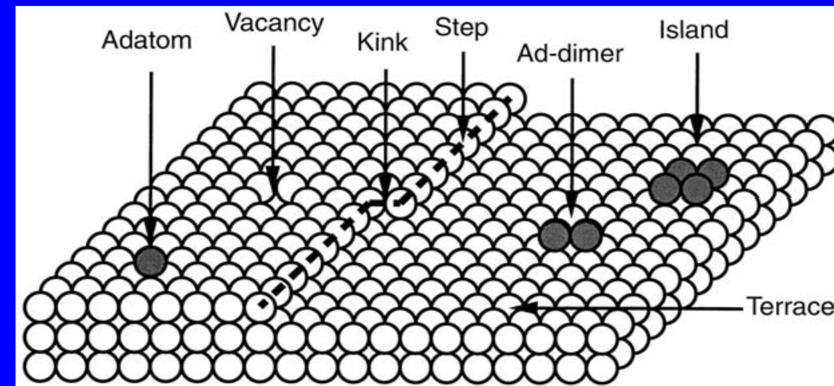

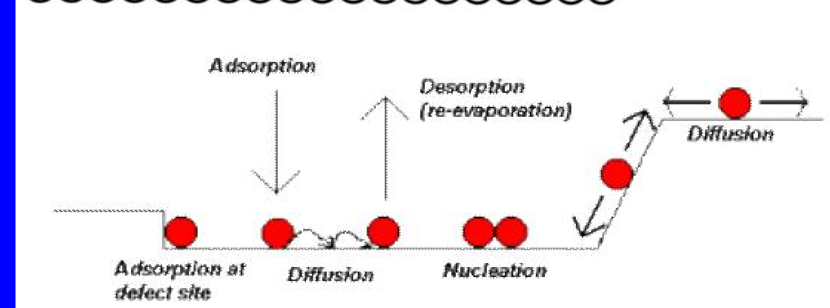

0.35 ML
30×30nm^2

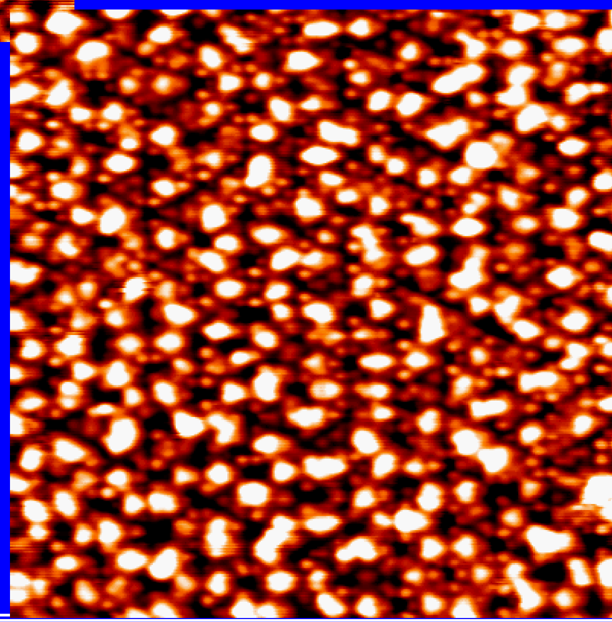

- Random distribution
- Irregular shape

Effect of Substrate Temperature

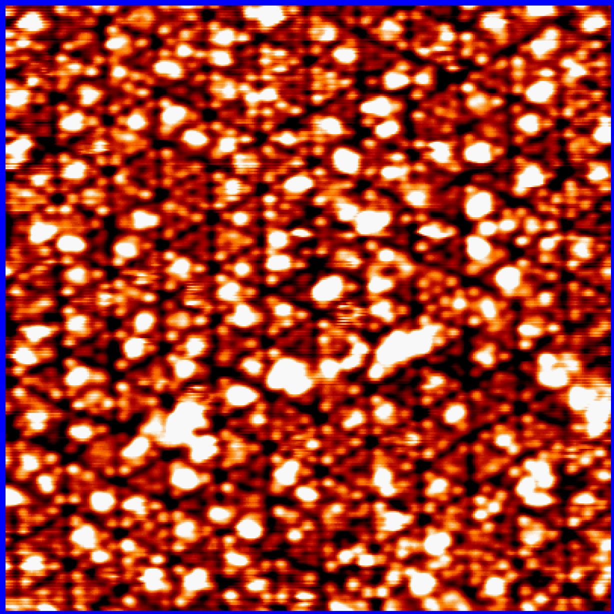

$30 \times 30 nm^2$@RT

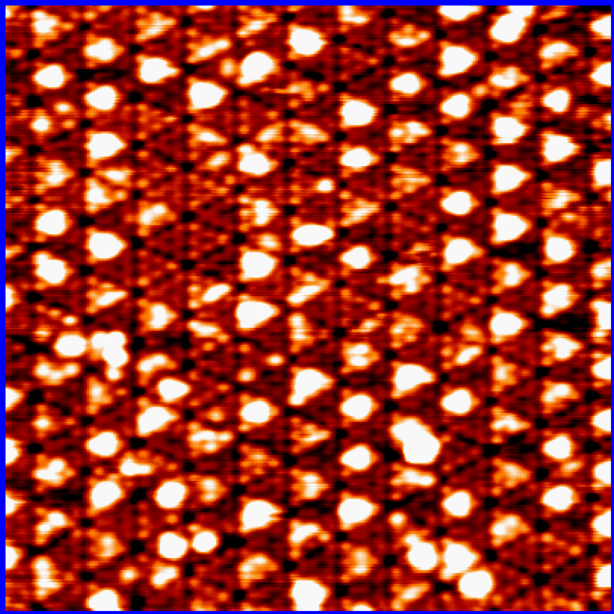

$30 \times 30 nm^2$@120^oC

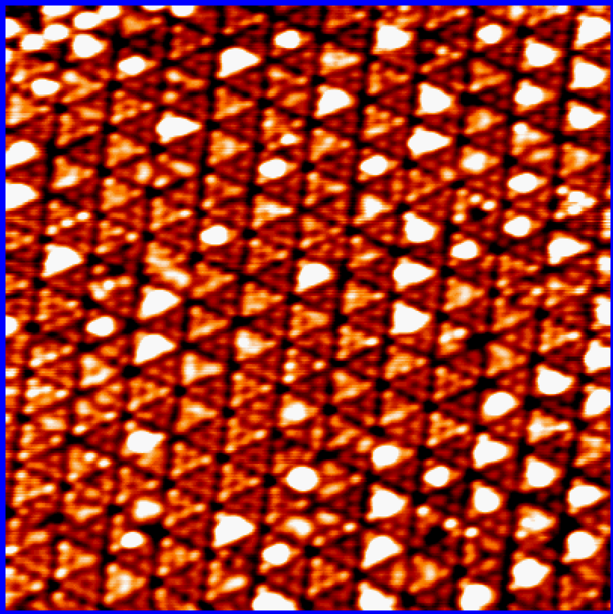

$30 \times 30 nm^2$@180^oC

Uniform Mn nanodots on Si(111)

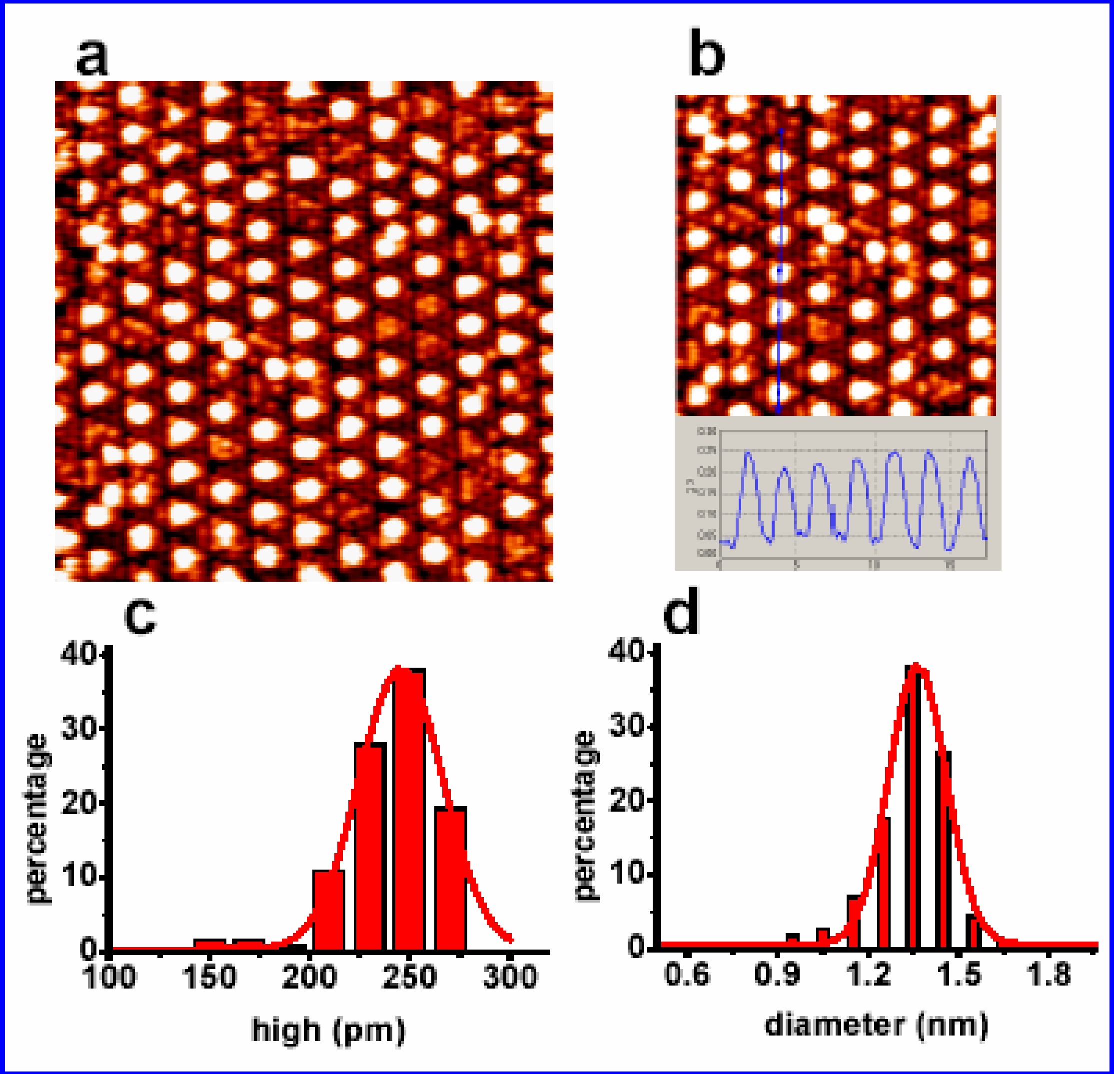

Uniform Mn nanodots on Si(111) with various coverage

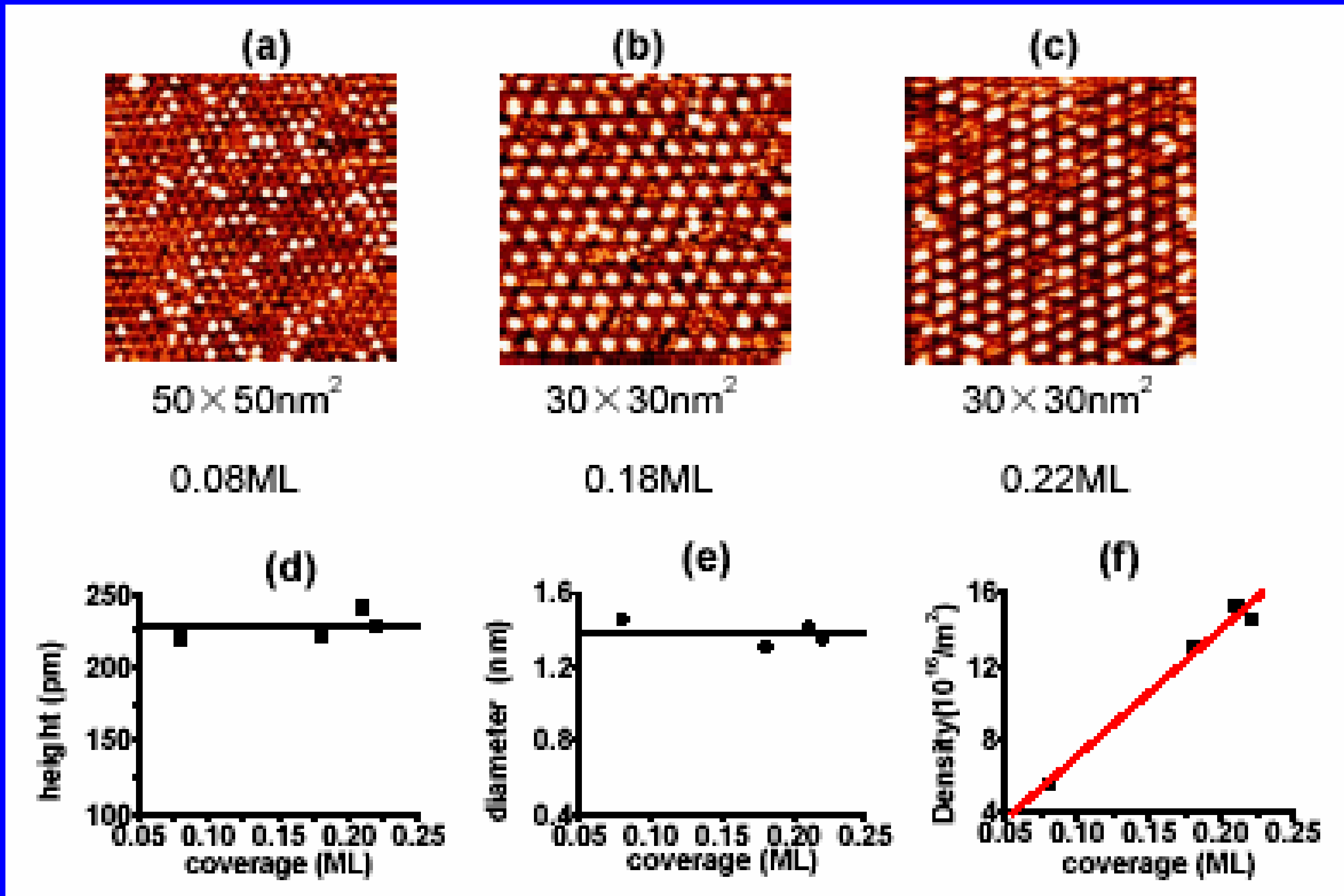

Preferential arrangement

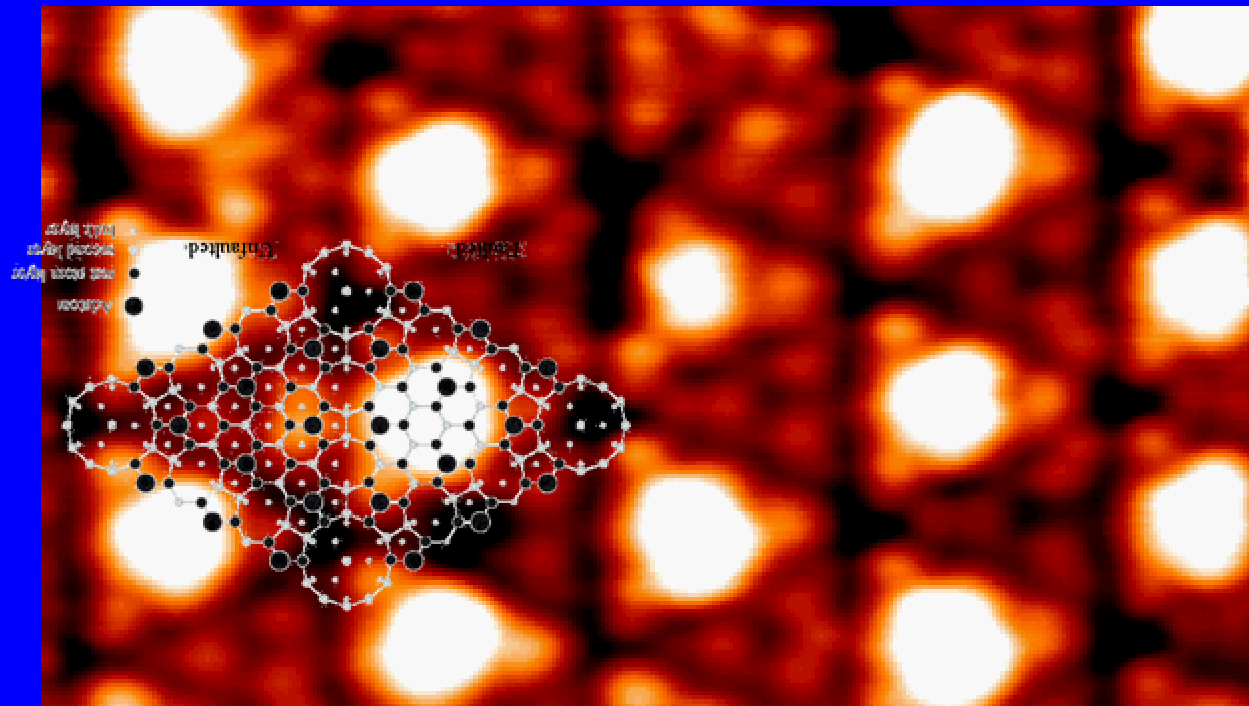

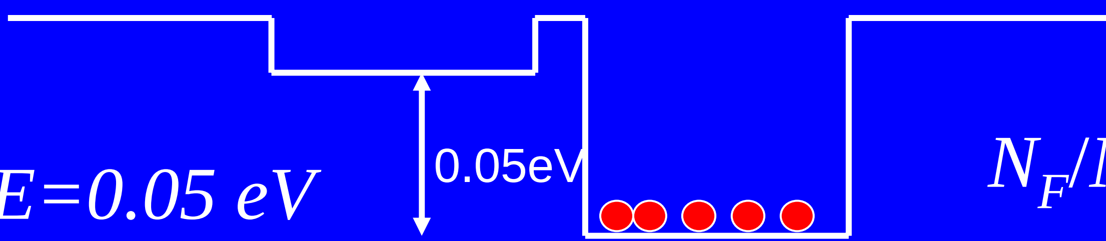

$\triangle E = 0.05\ eV$

$N_F/N_U=\exp(-\triangle E/k_BT)$

Effect of **deposition rate** on the proportion of Mn nanodots on unfaulted and faulted halves of Si(111)-7x7

0.167ML/min

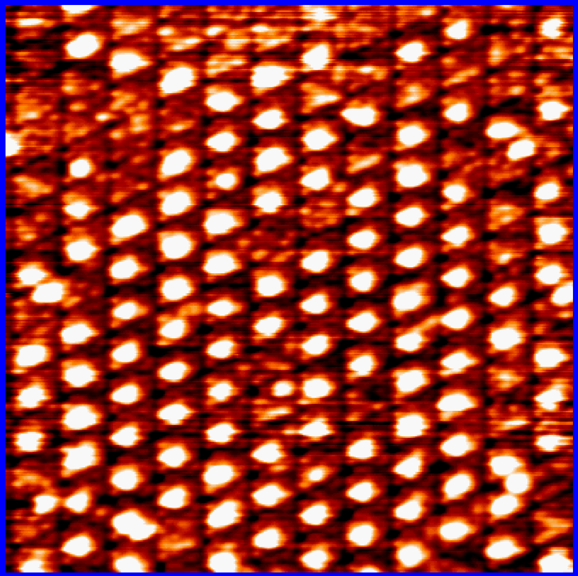

13.41ML/min

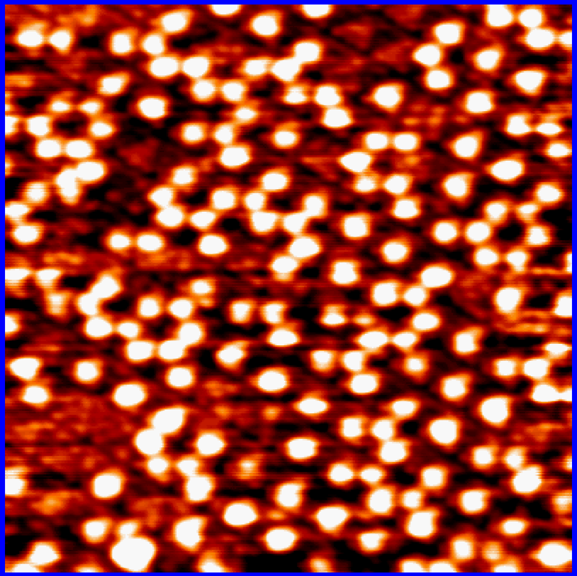

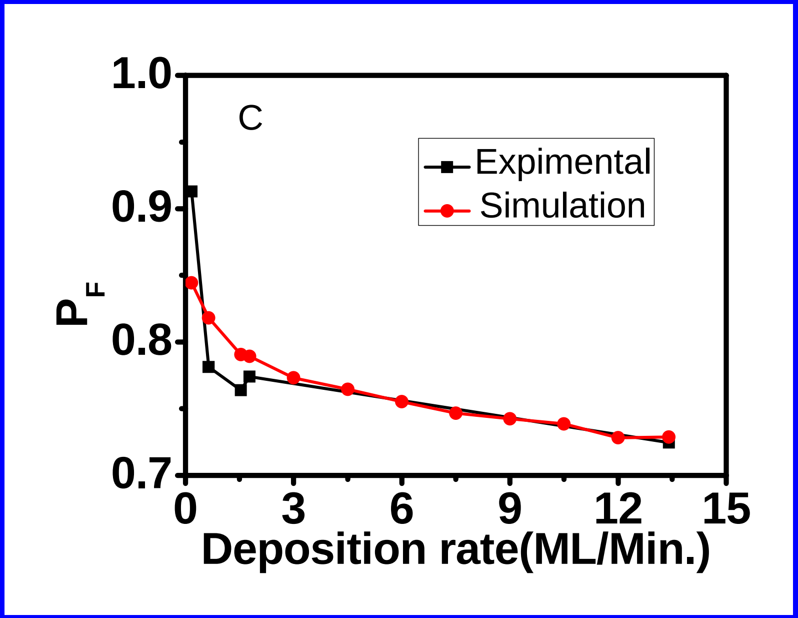

30×30nm^2@180 ^{o}C

II. Preferential arrangement and Controllable Growth of Mn Nanodots

Triangular structure

Honeycomb structure

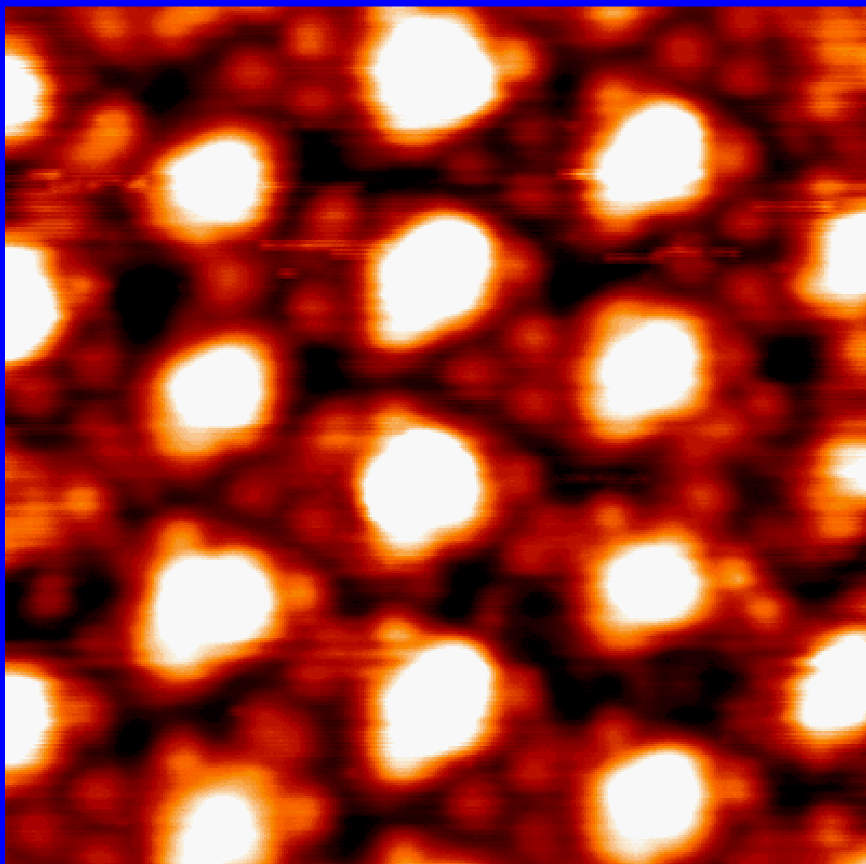

Deposition Rate

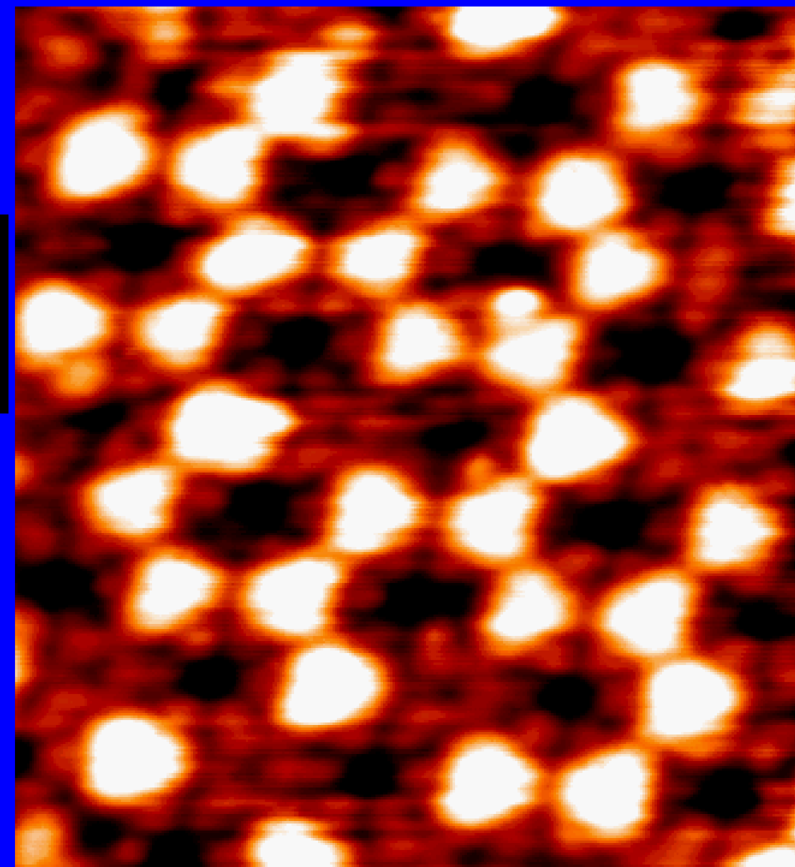

II. Preferential arrangement and Controllable Growth of Mn Nanodots

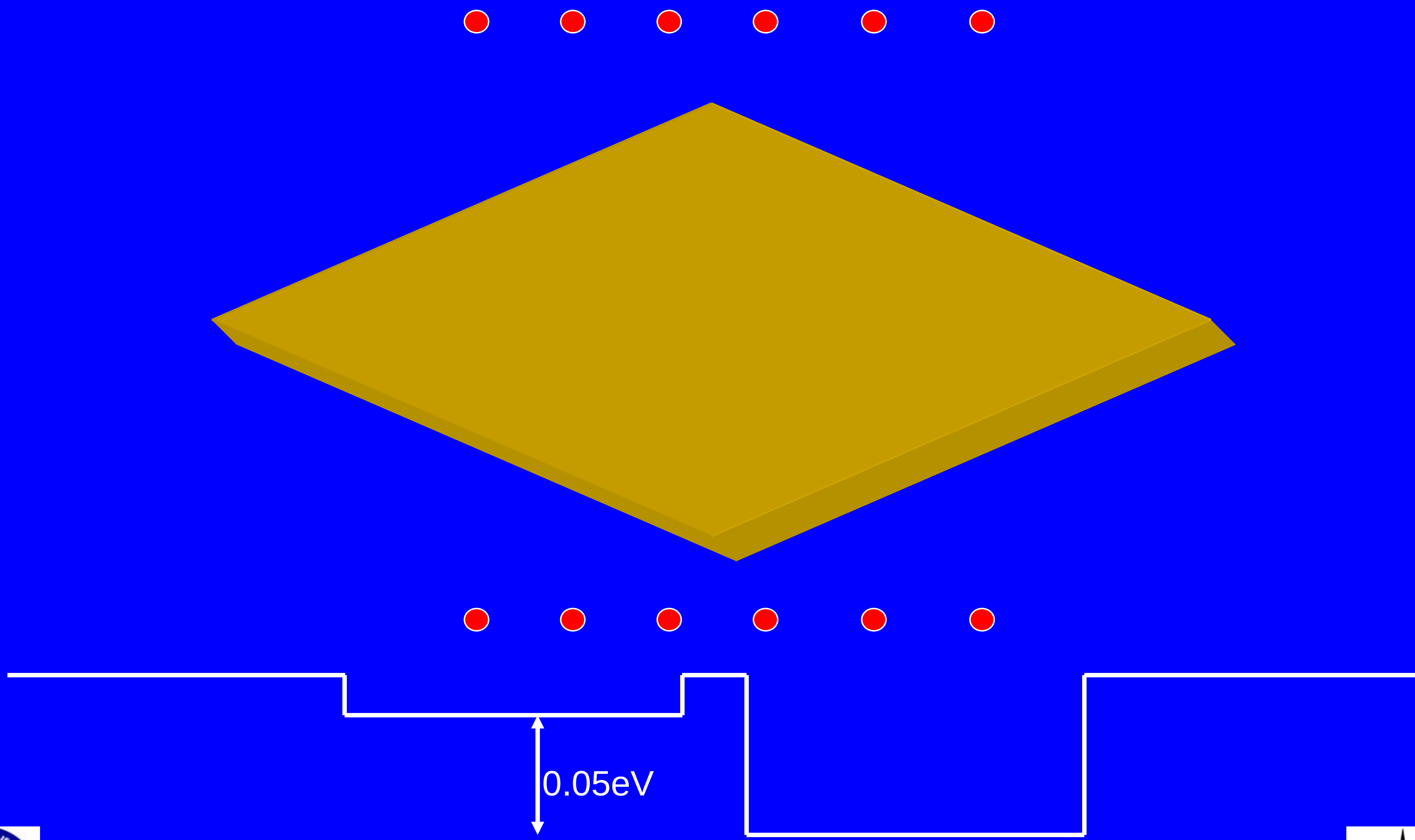

II. Preferential arrangement and Controllable Growth of Mn Nanodots

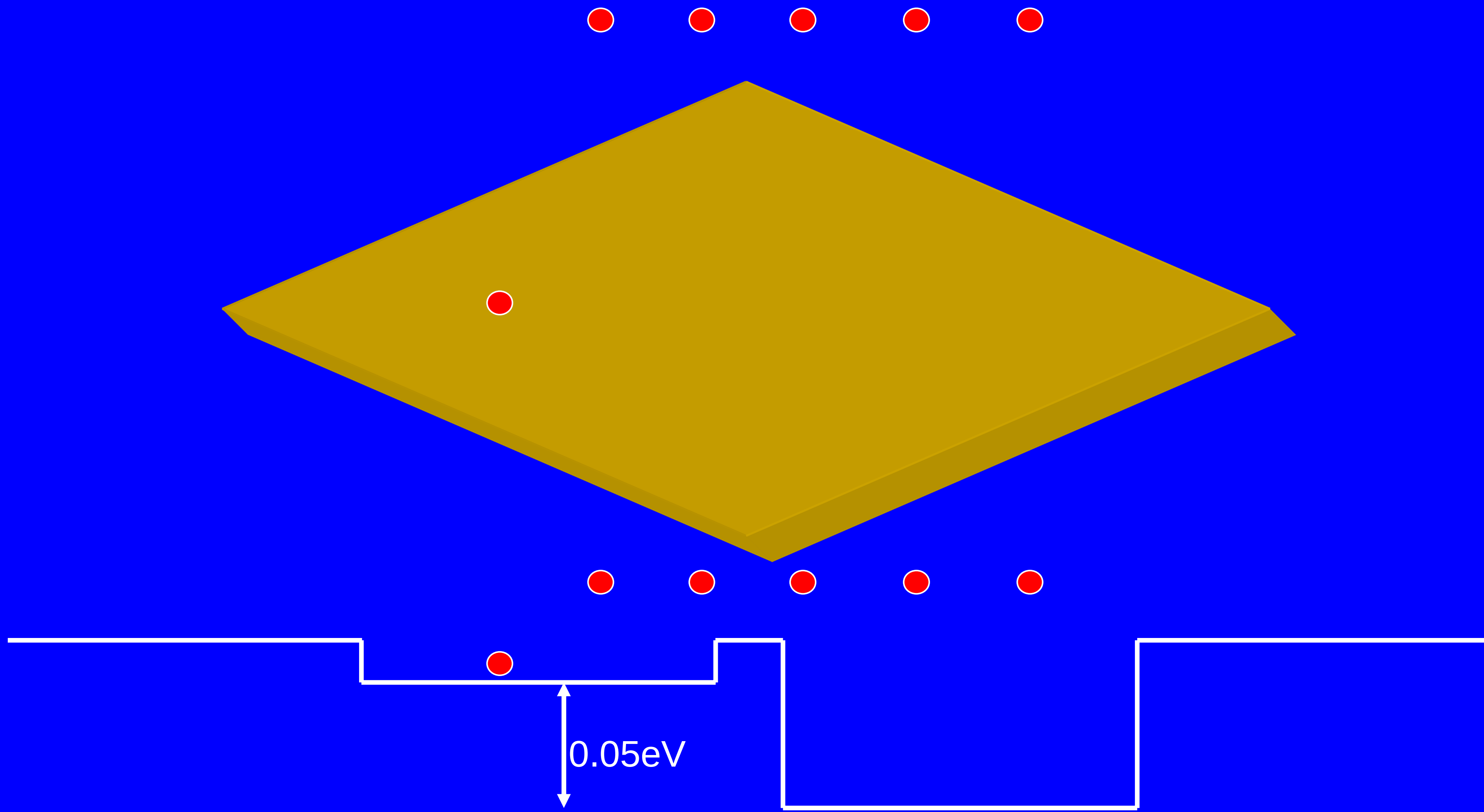

II. Preferential arrangement and Controllable Growth of Mn Nanodots

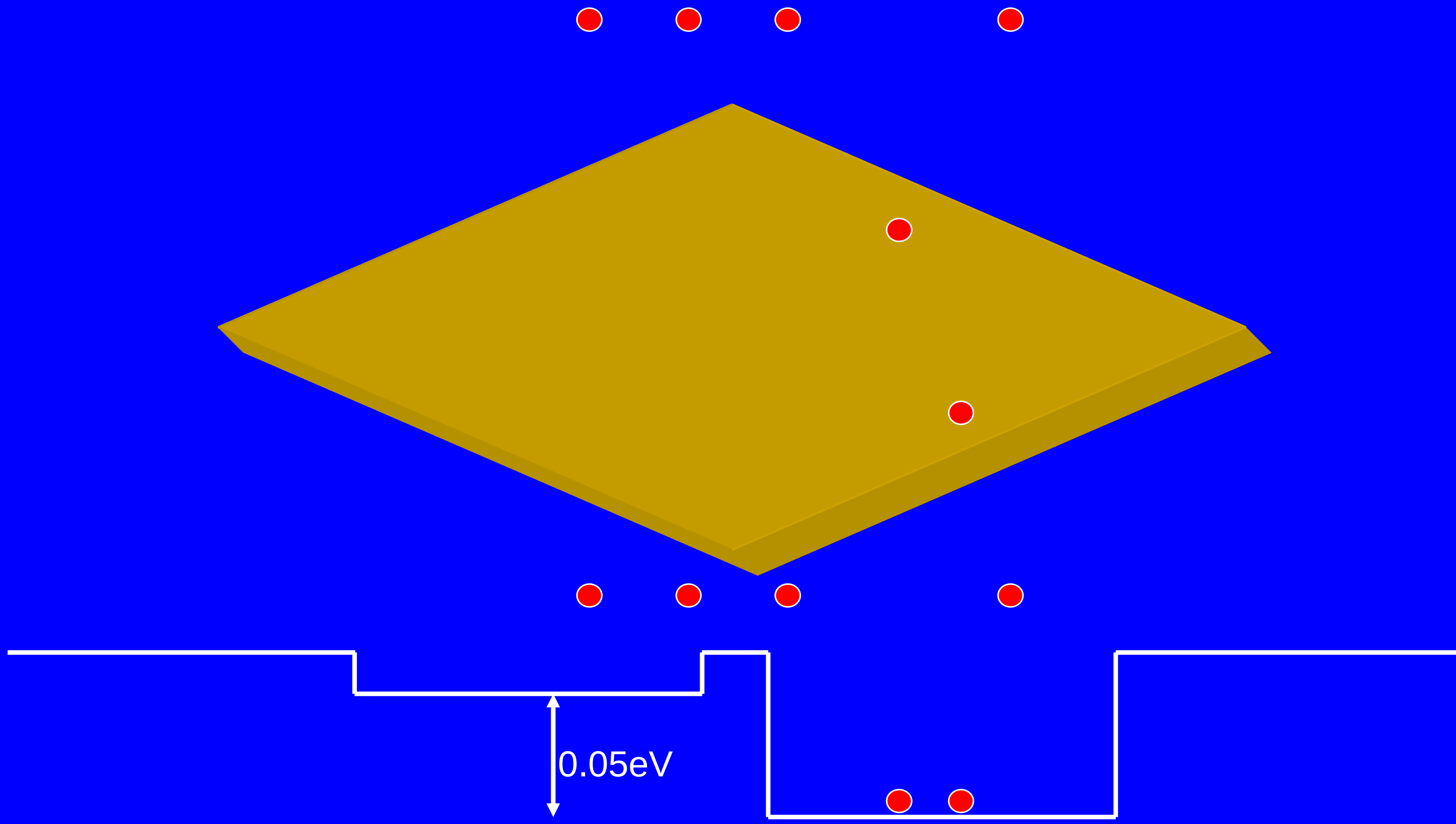

II. Preferential arrangement and Controllable Growth of Mn Nanodots

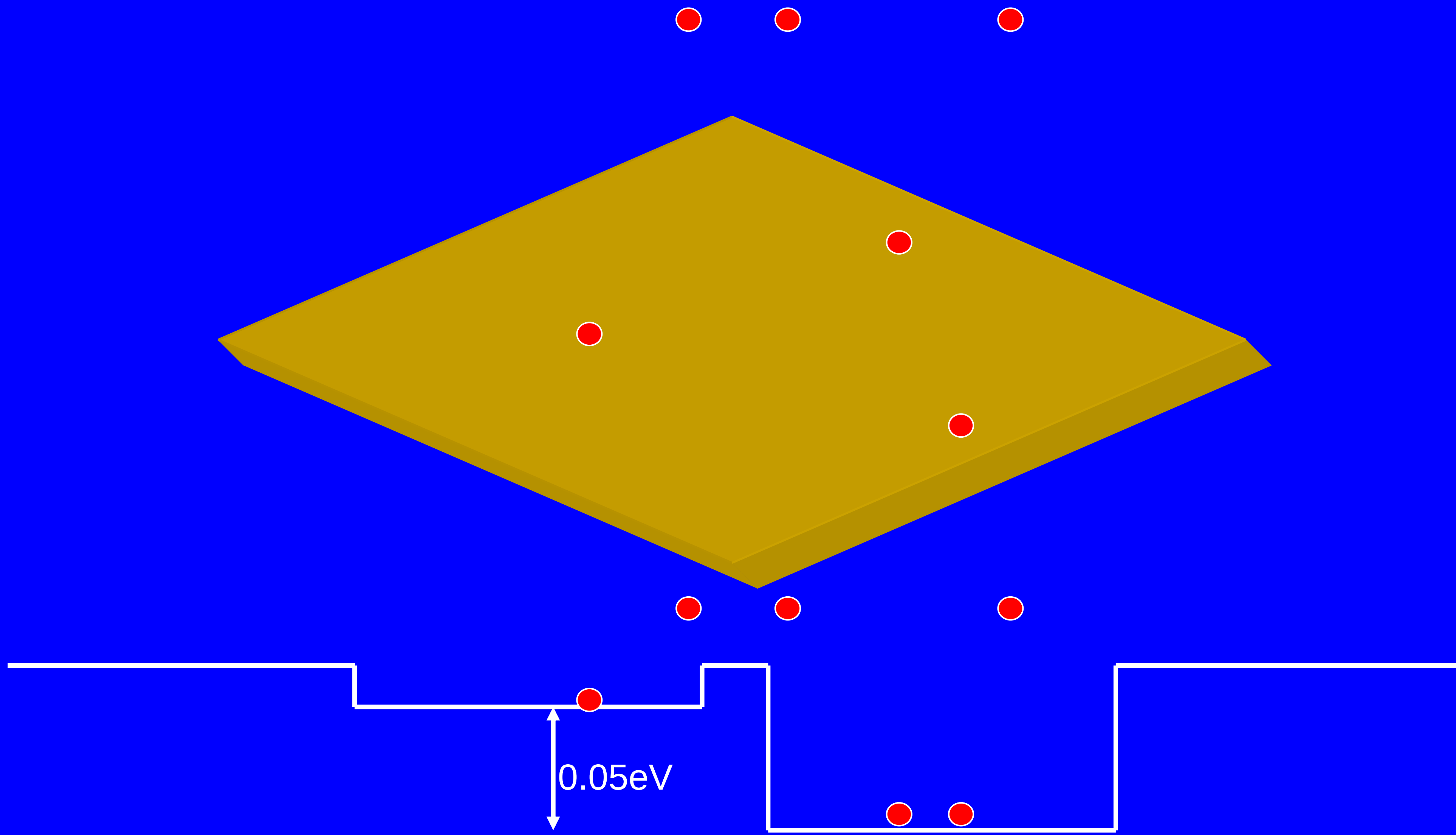

II. Preferential arrangement and Controllable Growth of Mn Nanodots

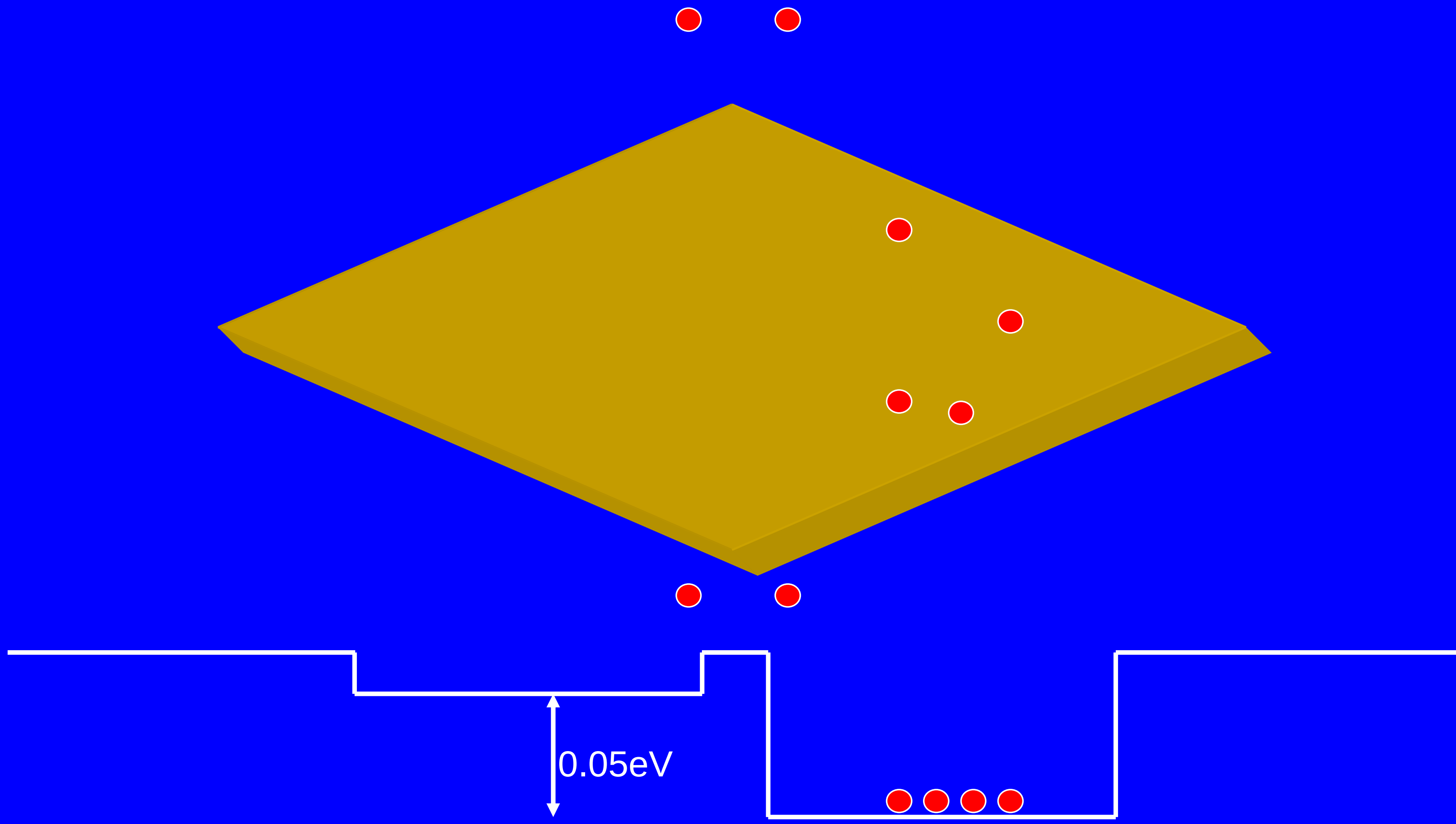

II. Preferential arrangement and Controllable Growth of Mn Nanodots

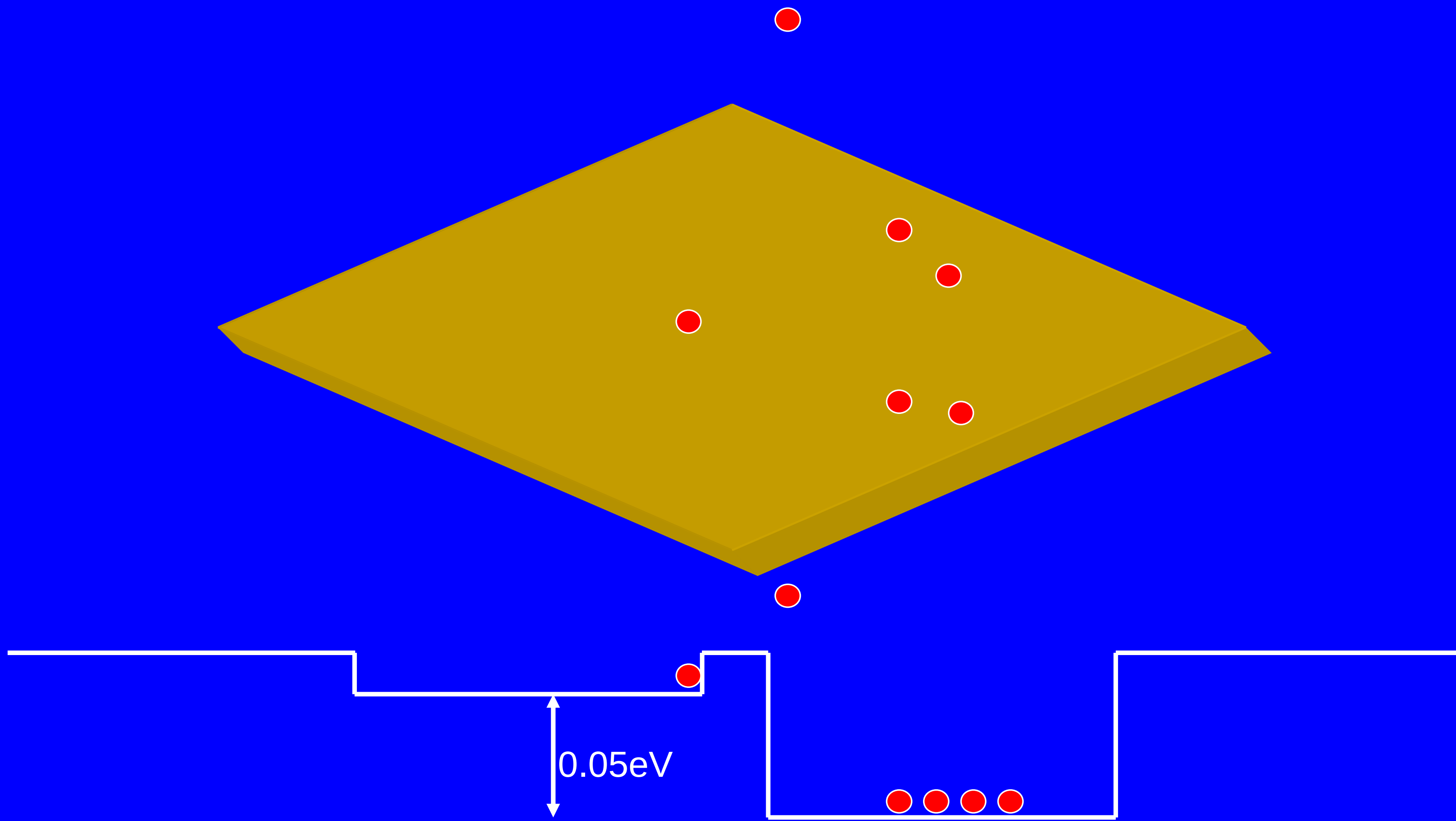

II. Preferential arrangement and Controllable Growth of Mn Nanodots

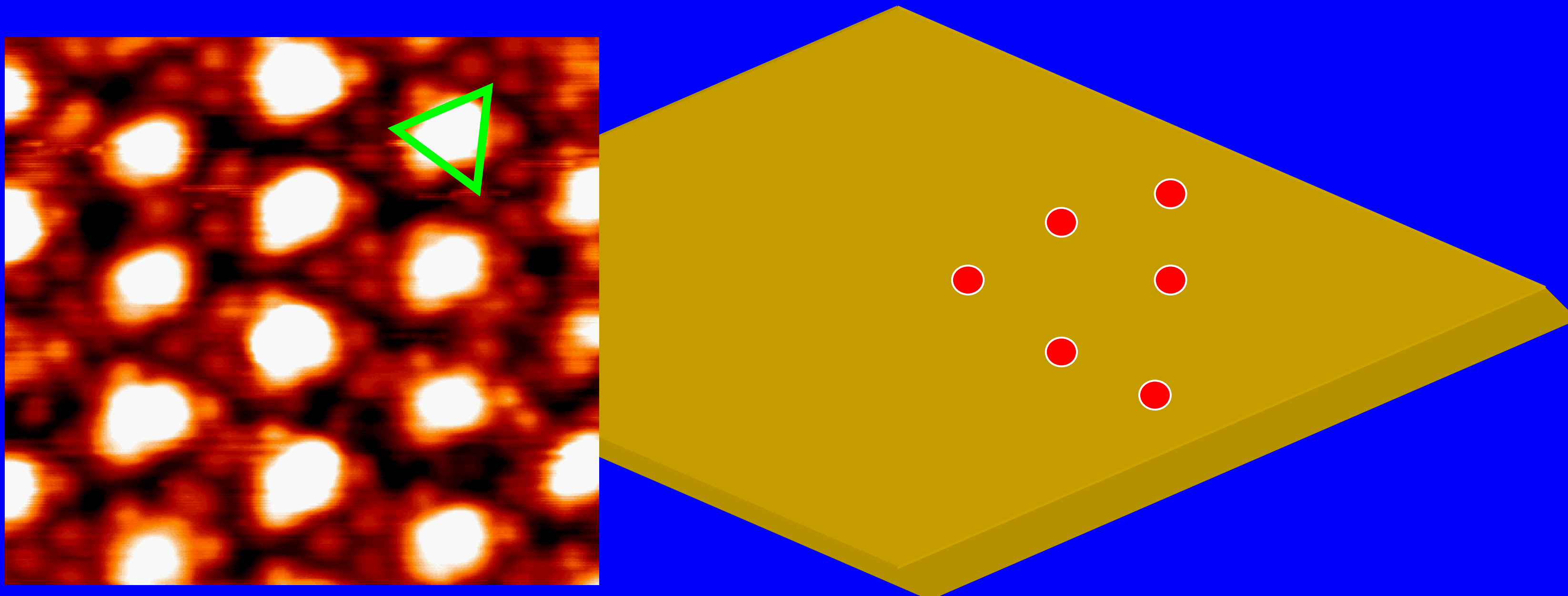

Explain

II. Preferential arrangement and Controllable Growth of Mn Nanodots

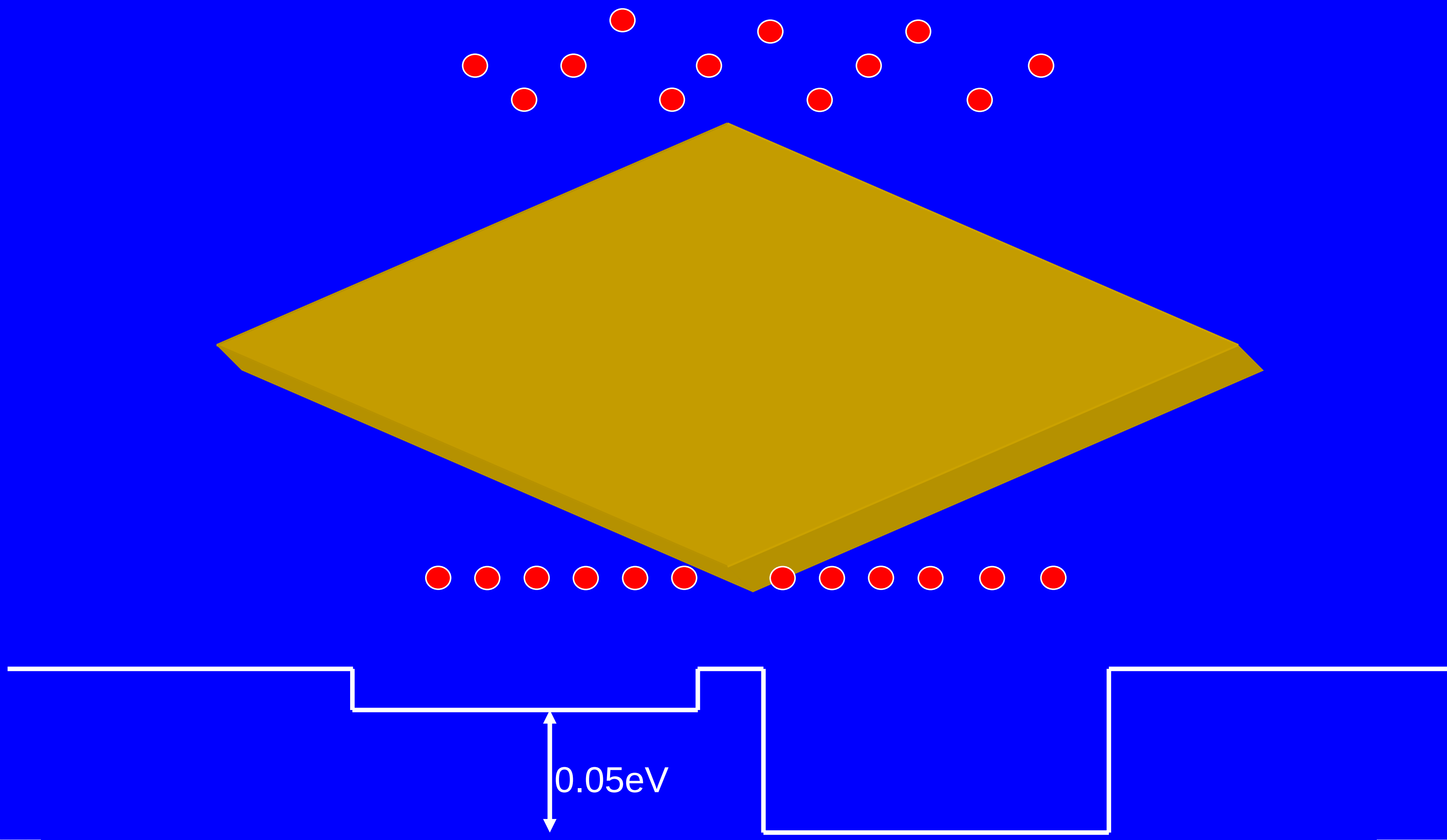

II. Preferential arrangement and Controllable Growth of Mn Nanodots

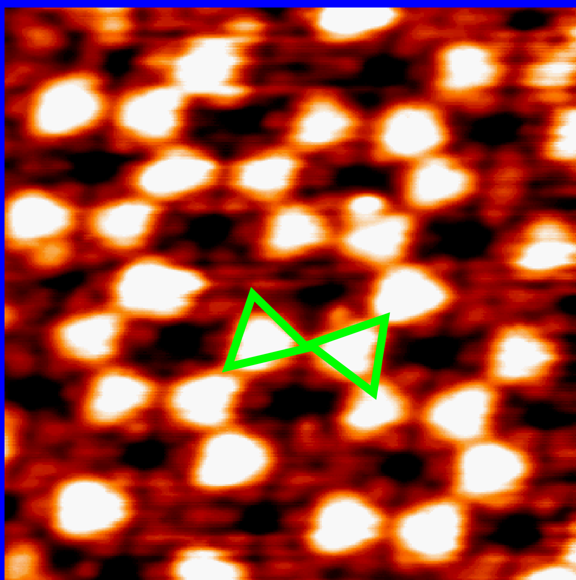

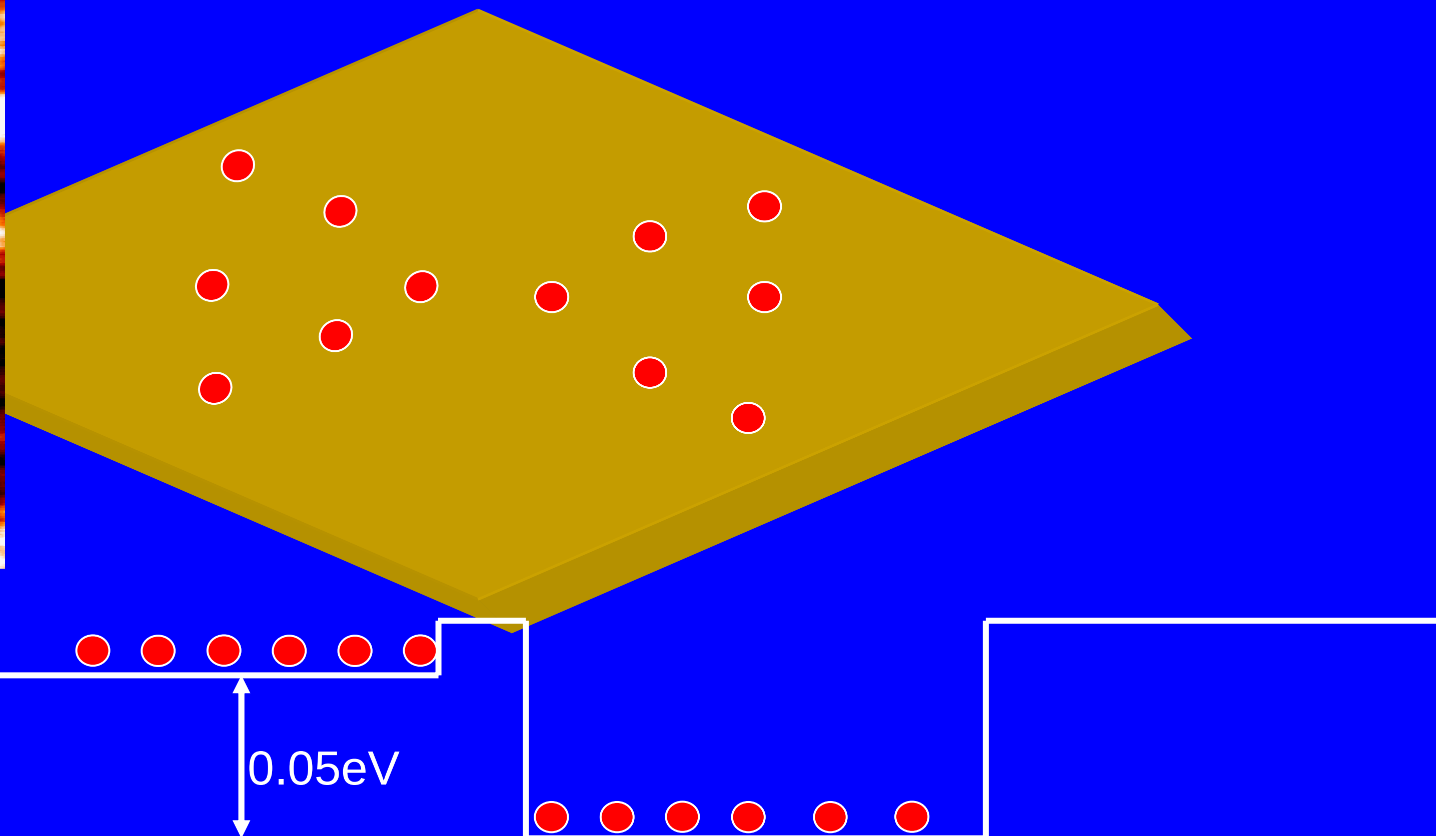

Kinetic Monte Carlo Simulation

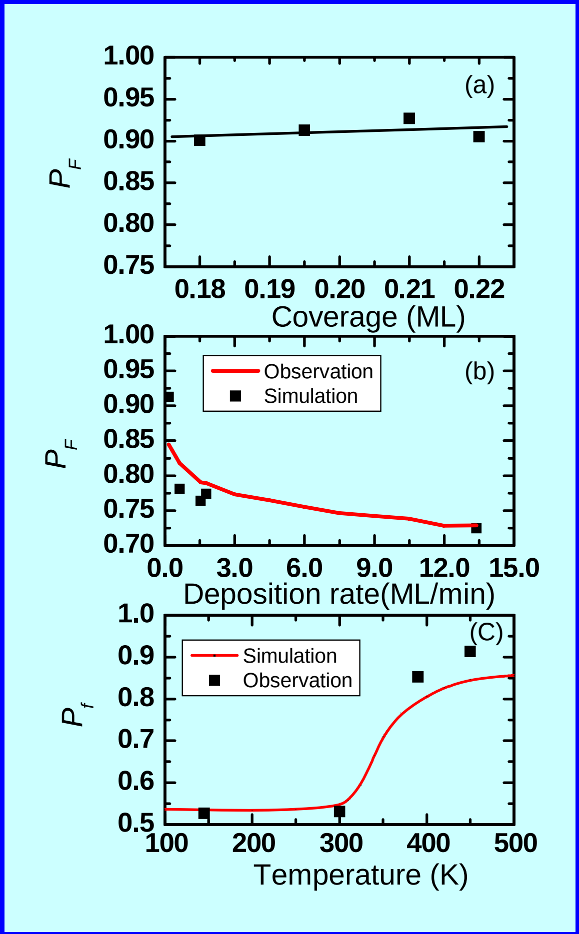

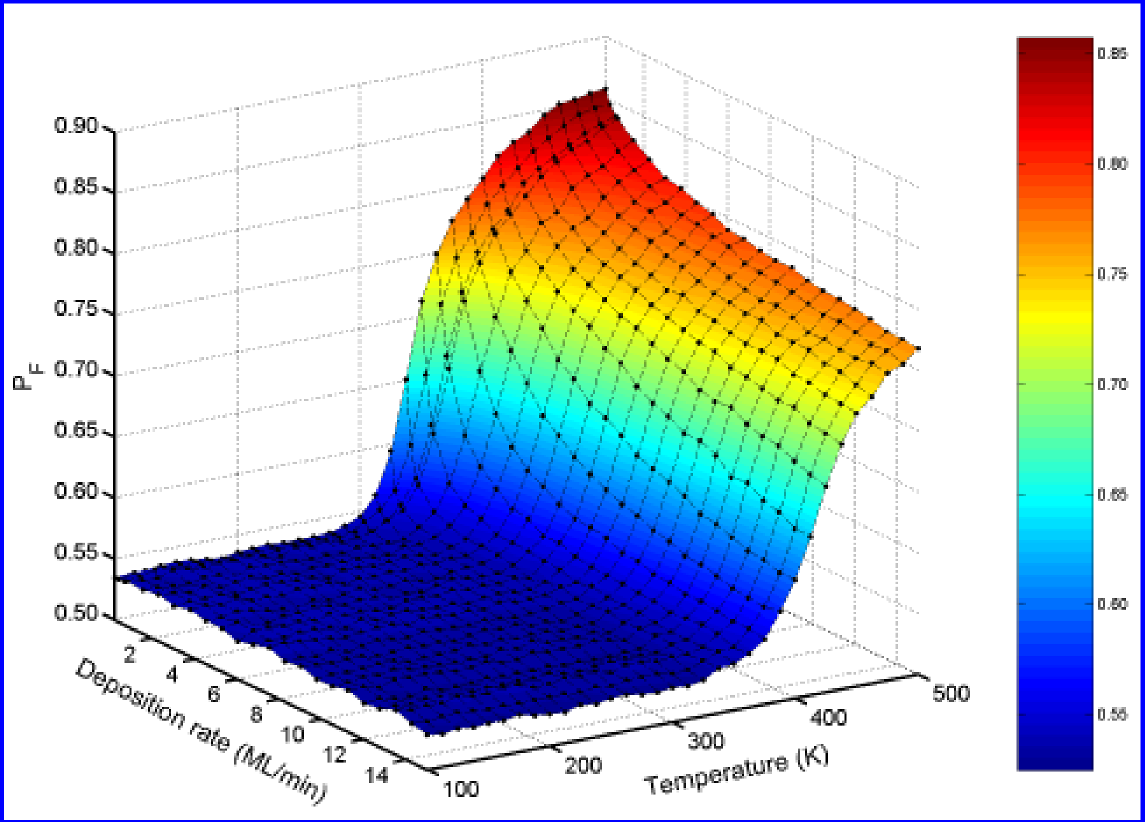

III. Fabrication of MnSi ultrathin film on Si(111)

0.02ML

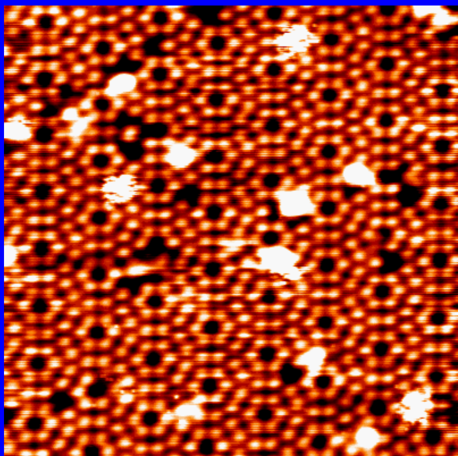

$250 \times 250 nm^2$

1.6ML

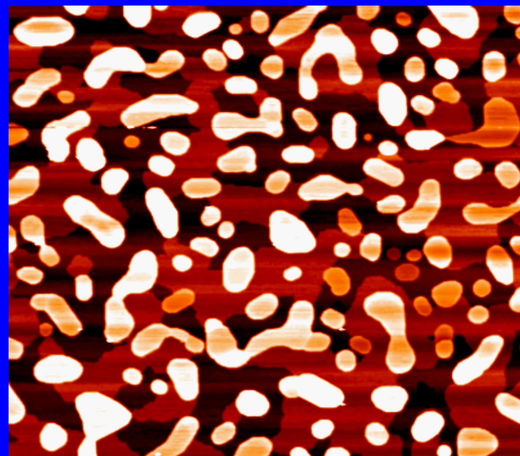

$250 \times 250 nm^2$

2.4ML

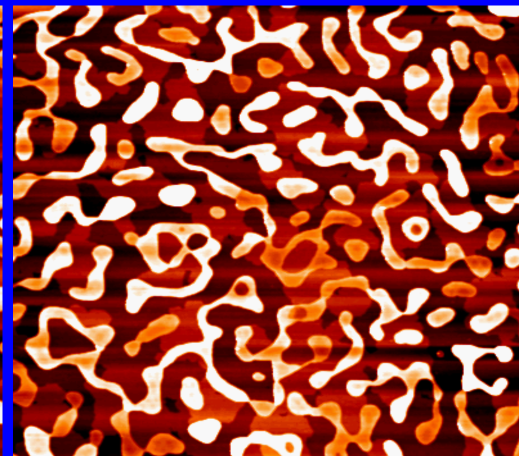

$1000 \times 1000 nm^2$

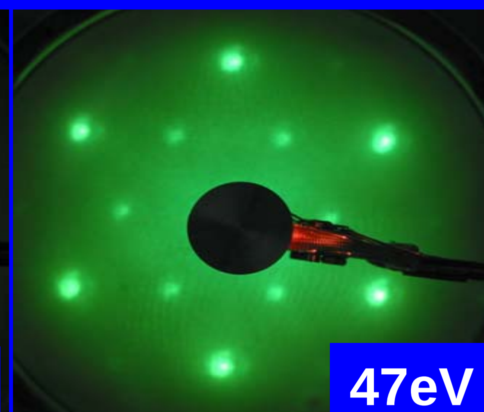

6ML

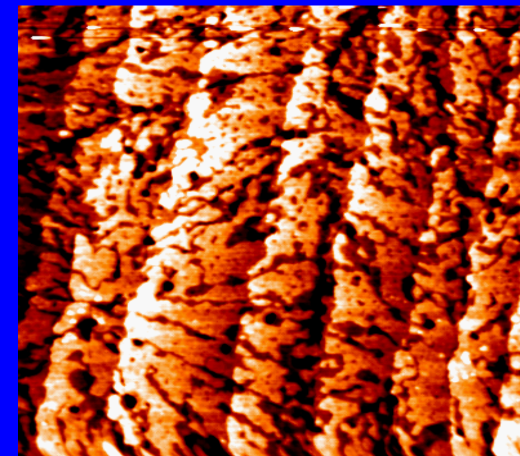

$1000 \times 1000 nm^2$

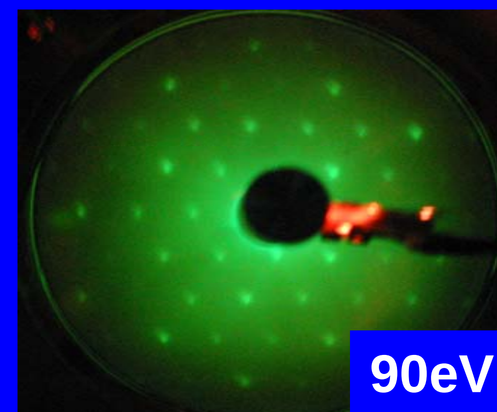

High Resolution STM image

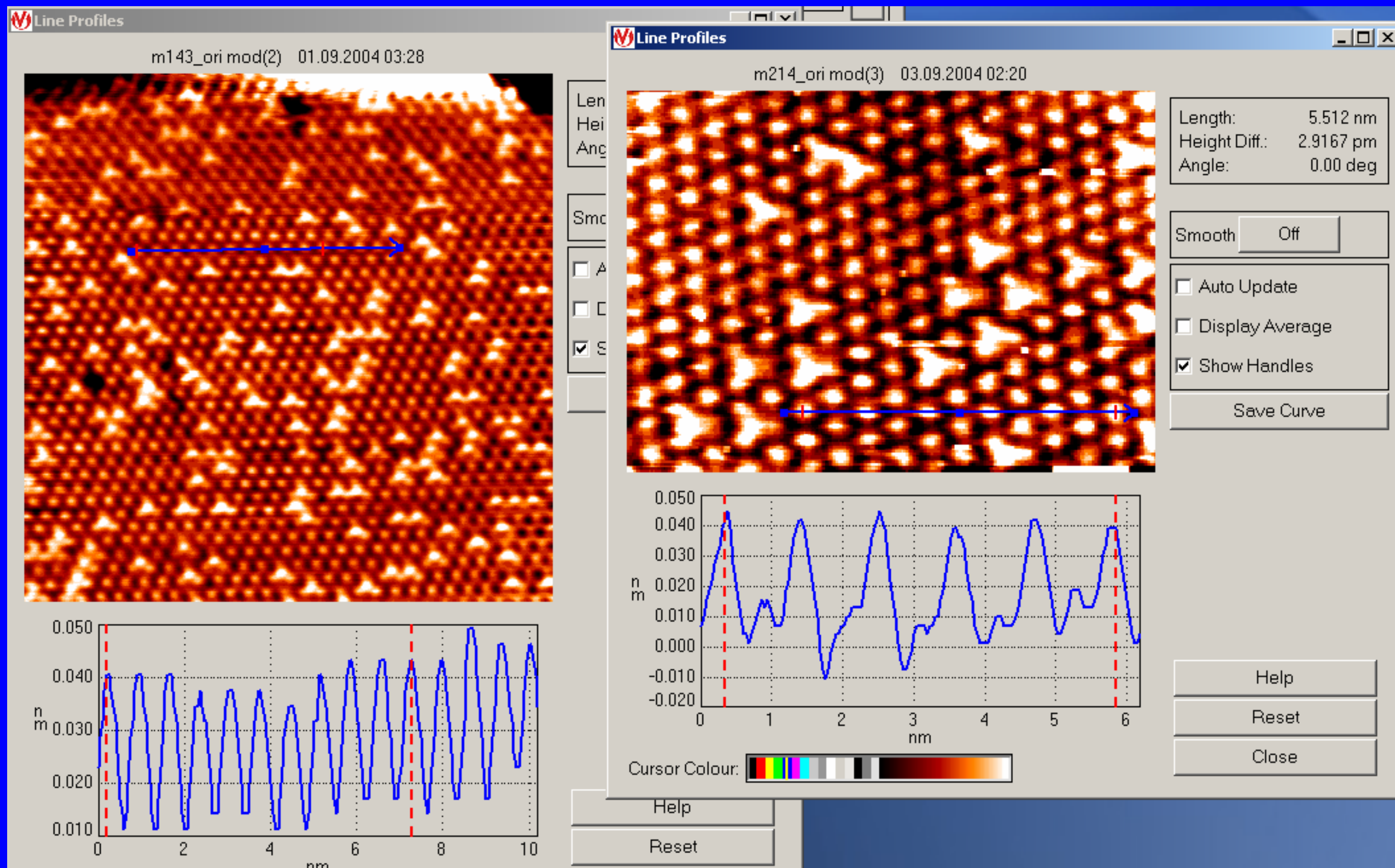

Distance in a $\sqrt{3}\times\sqrt{3}$ Reconstruction on Si(111) surface

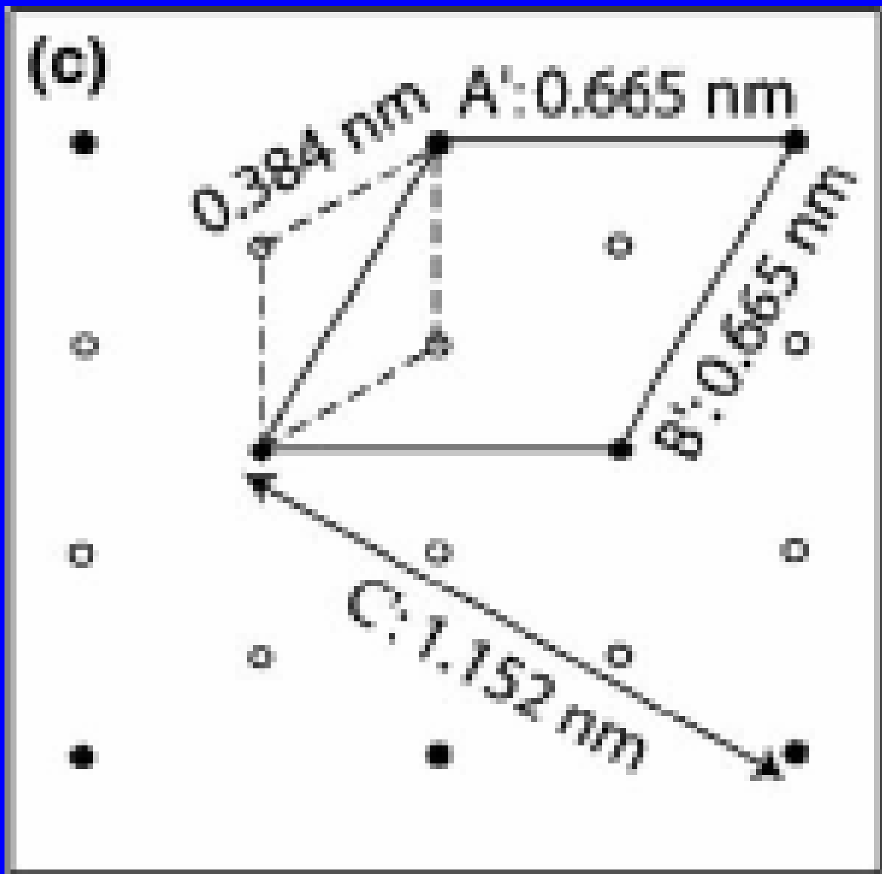

MnSi(111) surface:

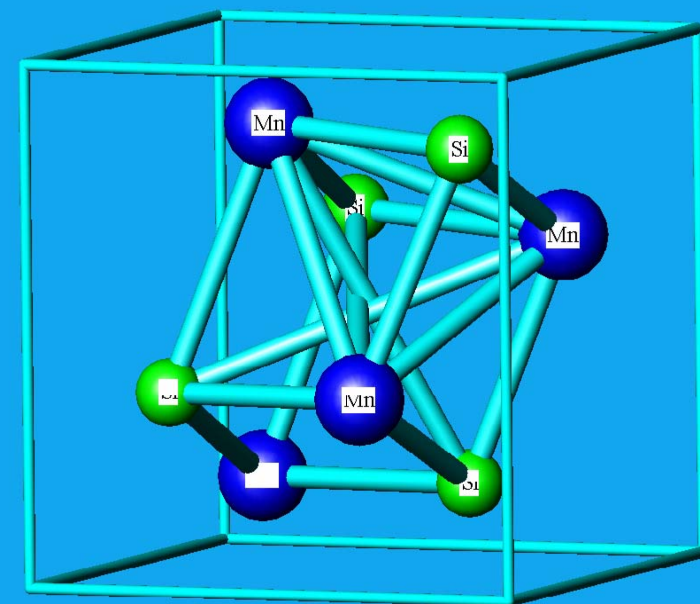

$d_{Mn\text{-}Si}=0.373$ nm

MnSi(111) surface:A=B=0.645nm,C=1.17nm

III. Fabrication of MnSi ultrathin film on Si(111)

Synchrotron XRD

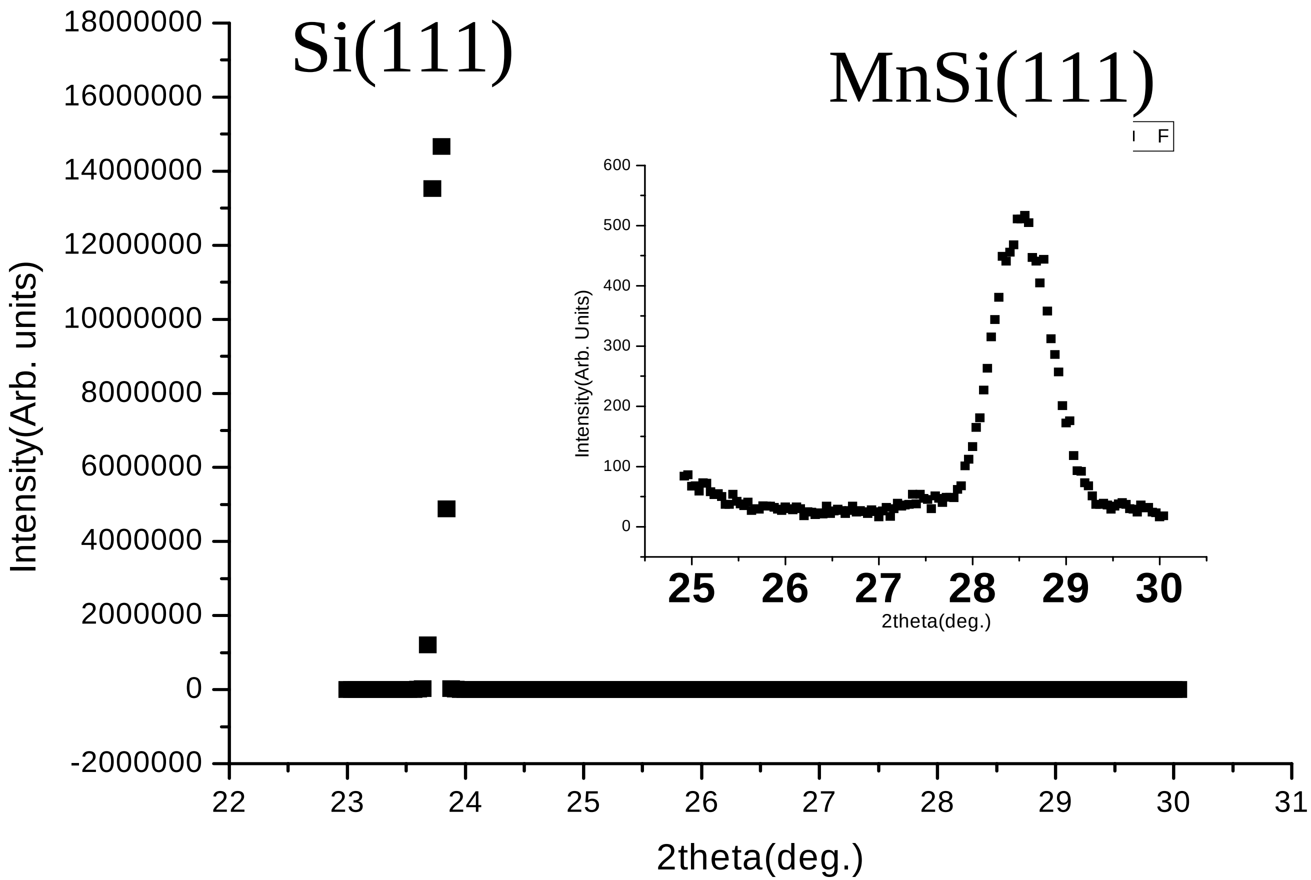

Growth model of MnSi

T. Nagao et al. / Surface Science 419 (1999) 134–143 139

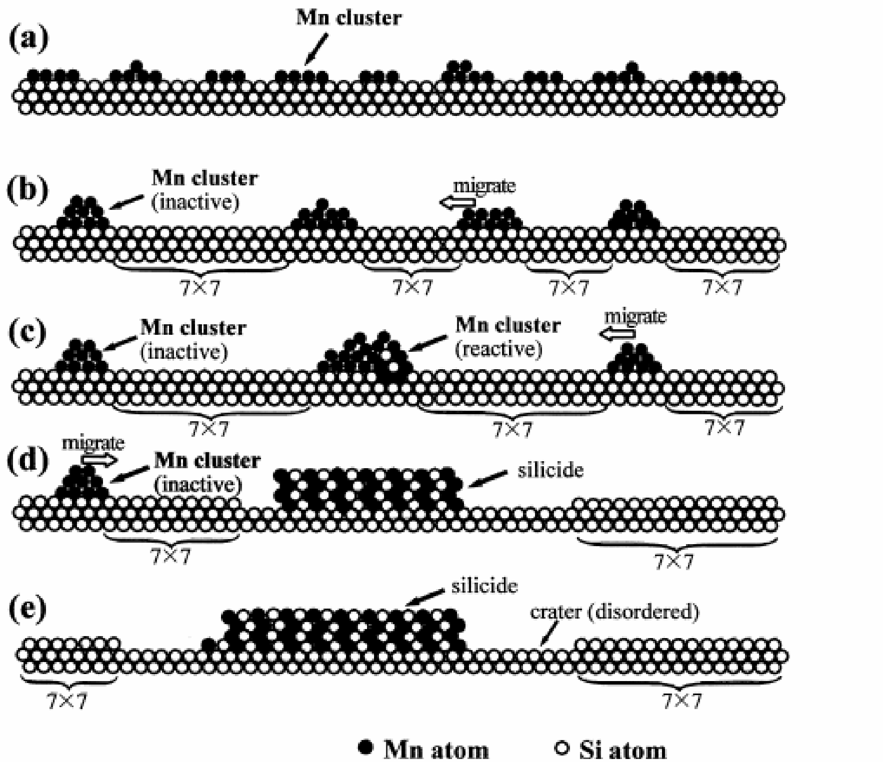

Fig. 3. Schematic illustrations for explaining the mechanism of Mn silicide formation on the Si(111)-(7×7) surface. ●, Mn atoms; ○, Si atoms.

T. Nagao et al., Surf. Sci. 419(1999), 134

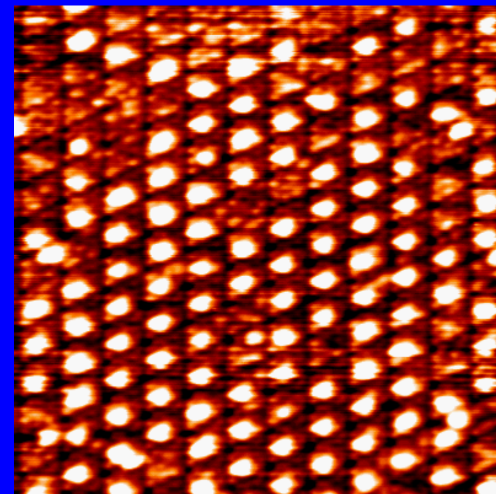

As-deposited

30×30nm^2

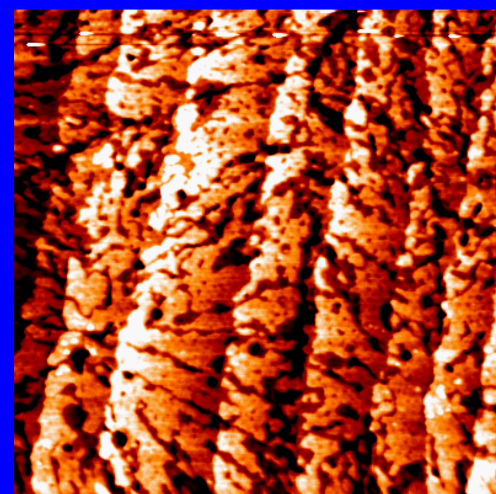

Post-annealed

1000×1000nm^2

IV. Magnetic and Magnetotransport Properties of MnSi Ultrathin films

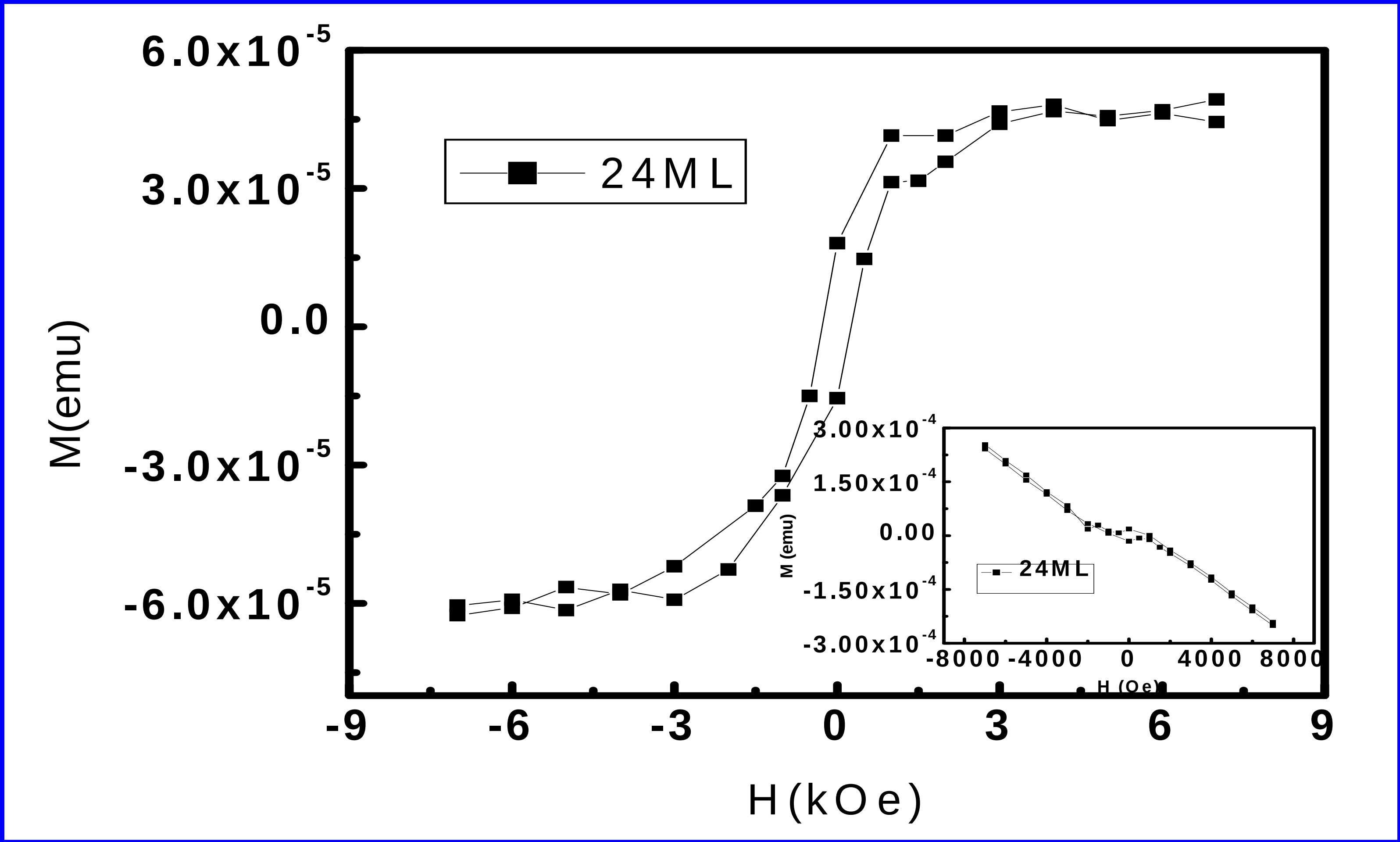

IV. Magnetic and Magnetotransport Properties of MnSi Ultrathin films

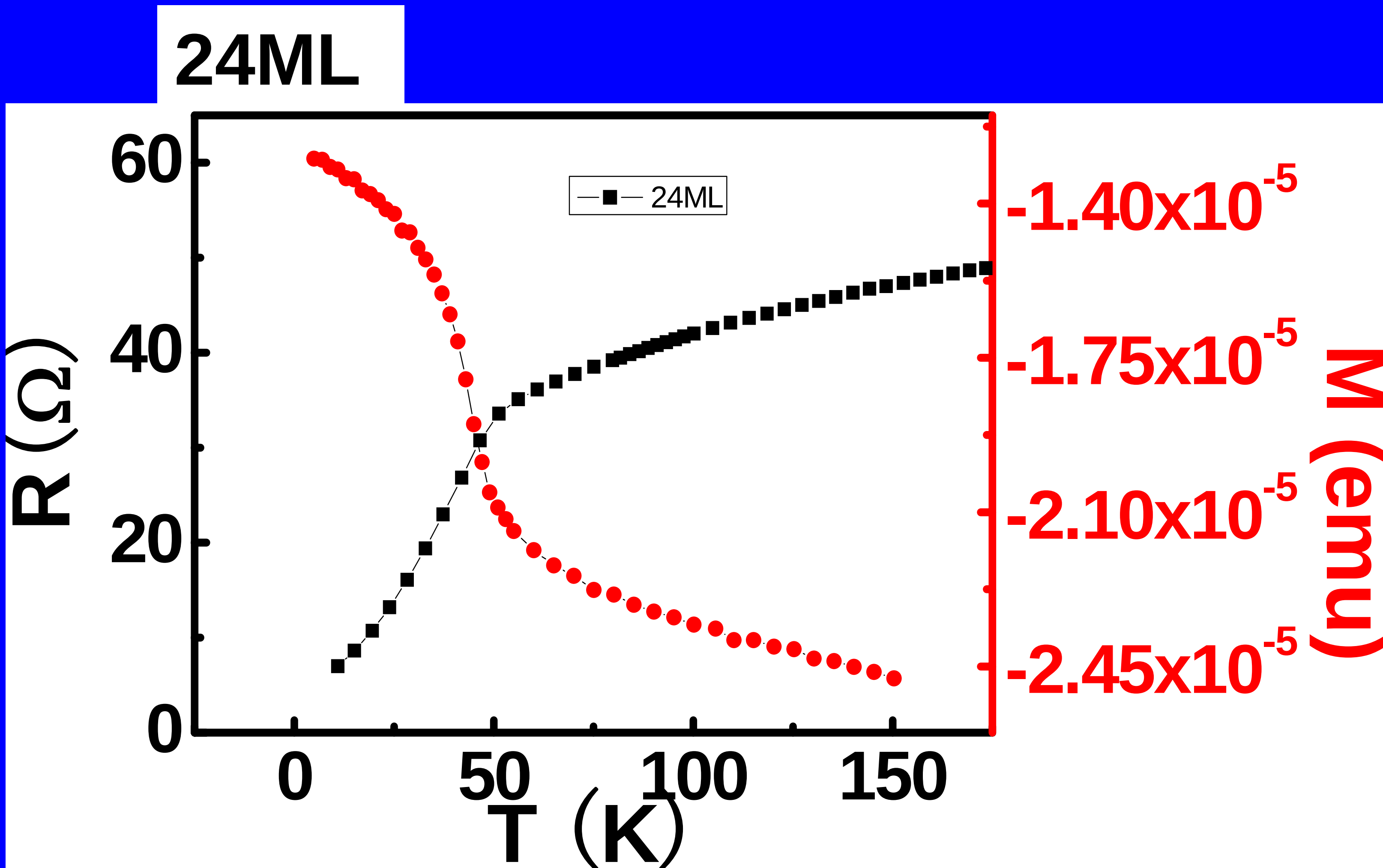

III. Magnetic and Magnetotransport Properties of MnSi Ultrathin films

Enhancement of Tc

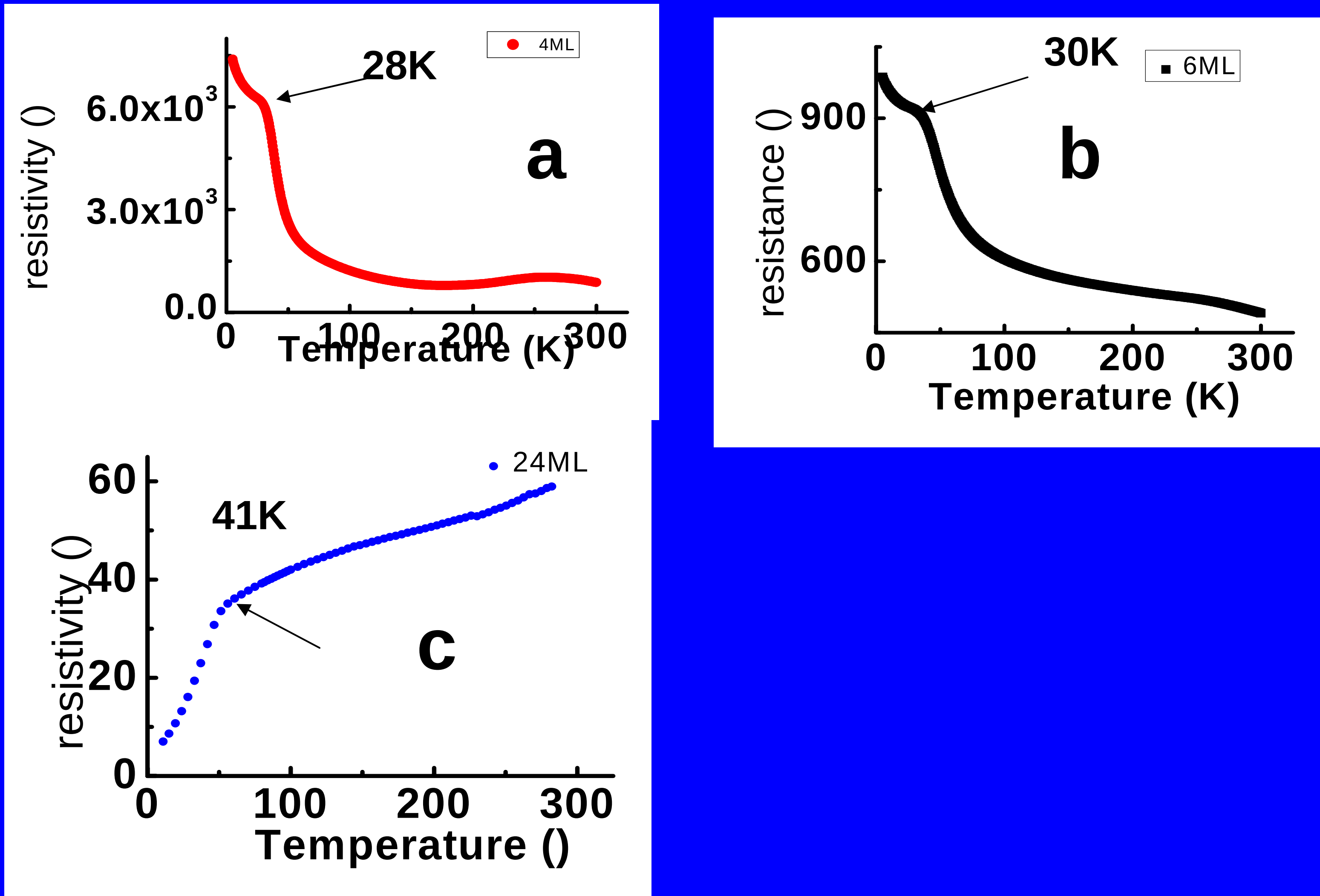

Enhancement of Tc

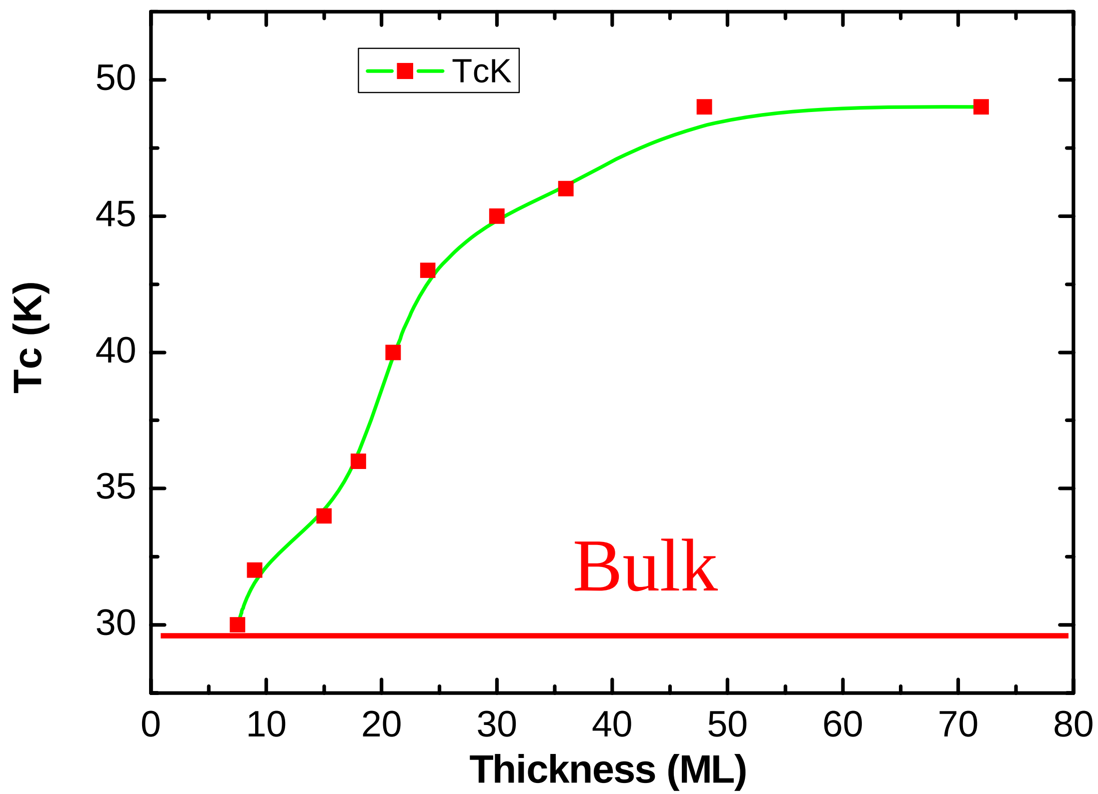

Pressure effect on Tc

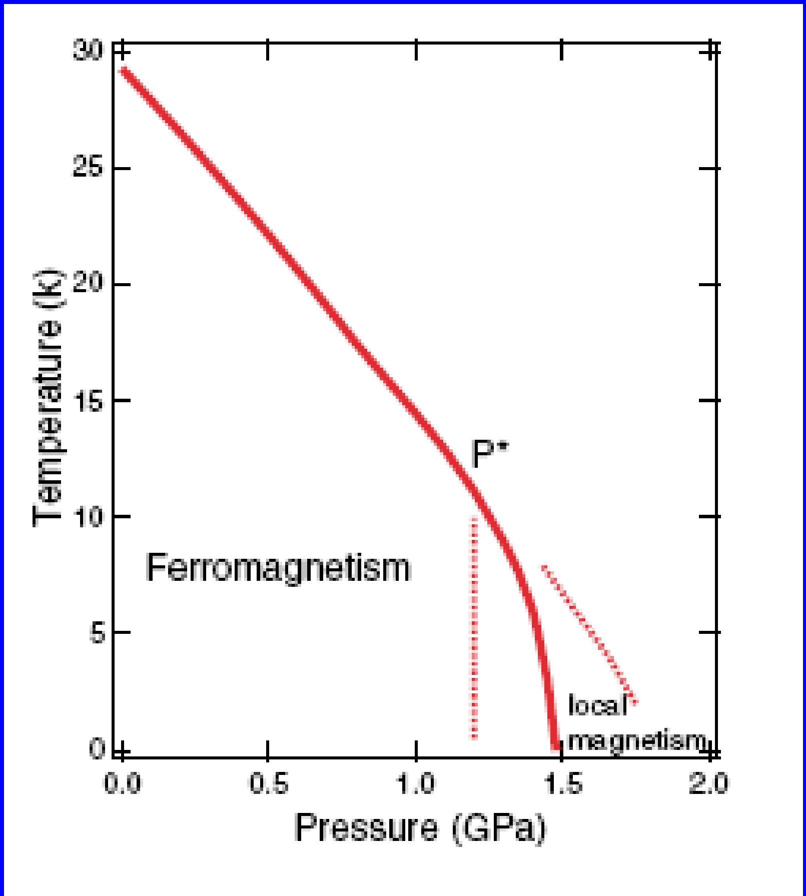

W. Yu et al., PRL, 92,086403(2004)

Enhancement of Tc

driven by epitaxial strain ?

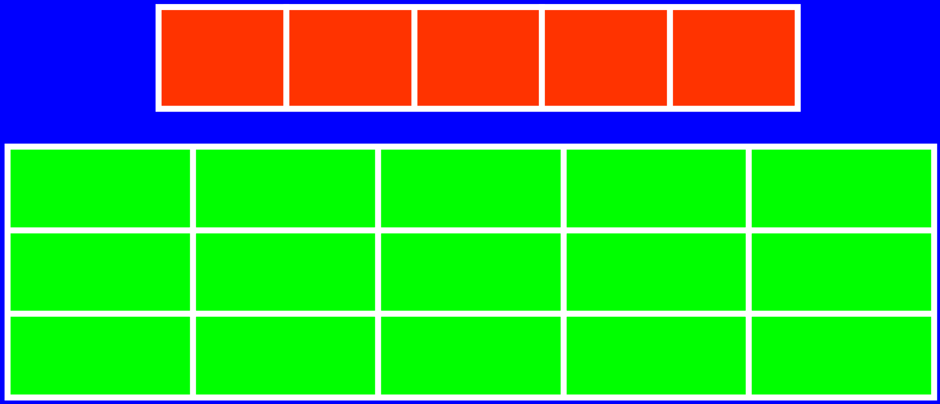

Enhancement of Tc

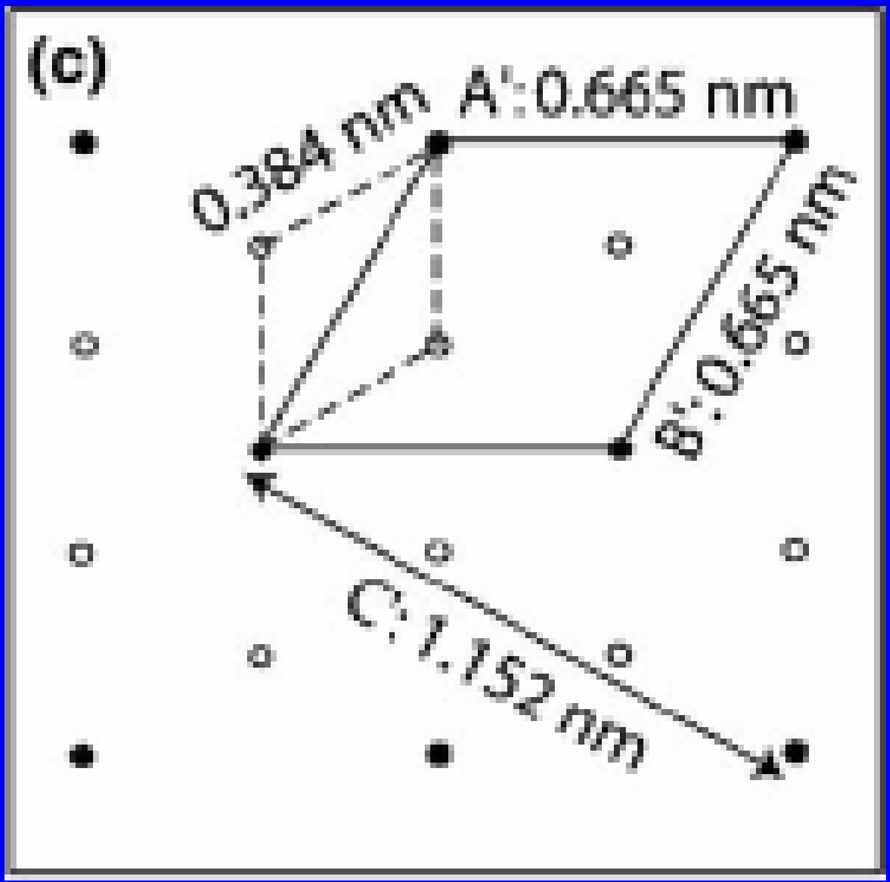

MnSi(111) surface:

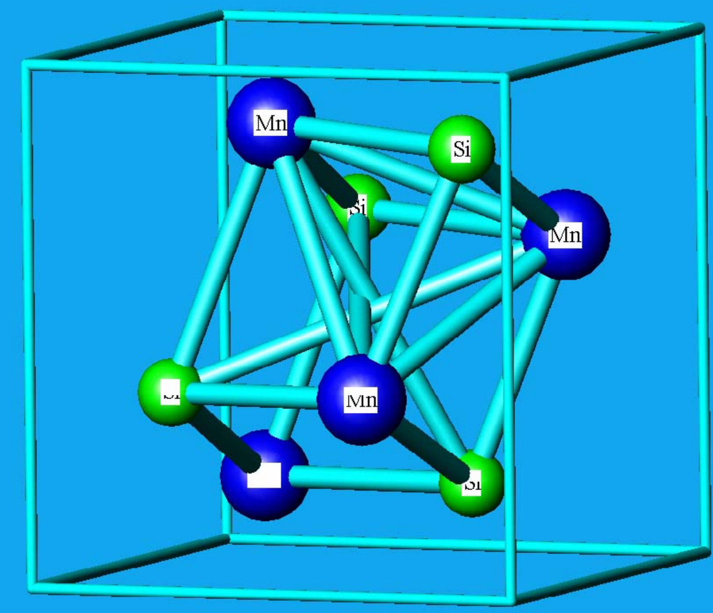

$d_{Mn\text{-}Si}=0.373$ nm

MnSi(111) surface:A=B=0.645nm,C=1.17nm

Enhancement of Tc

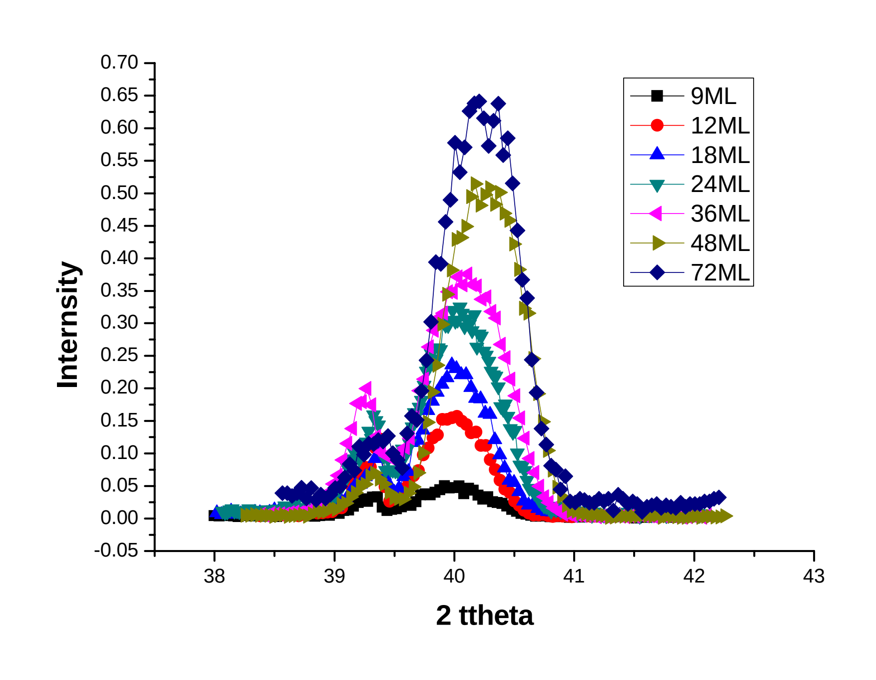

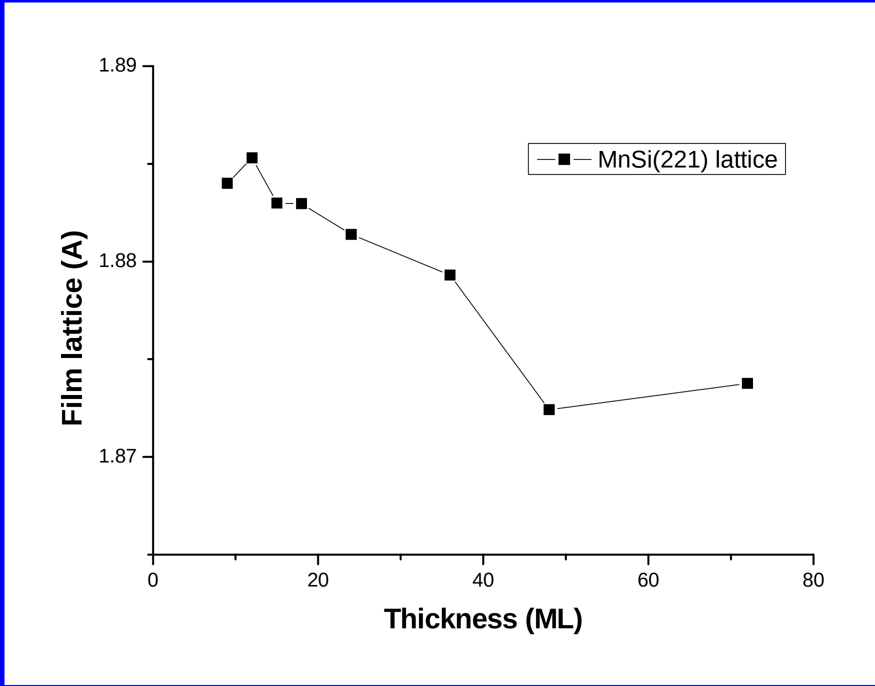

Enhancement of Tc

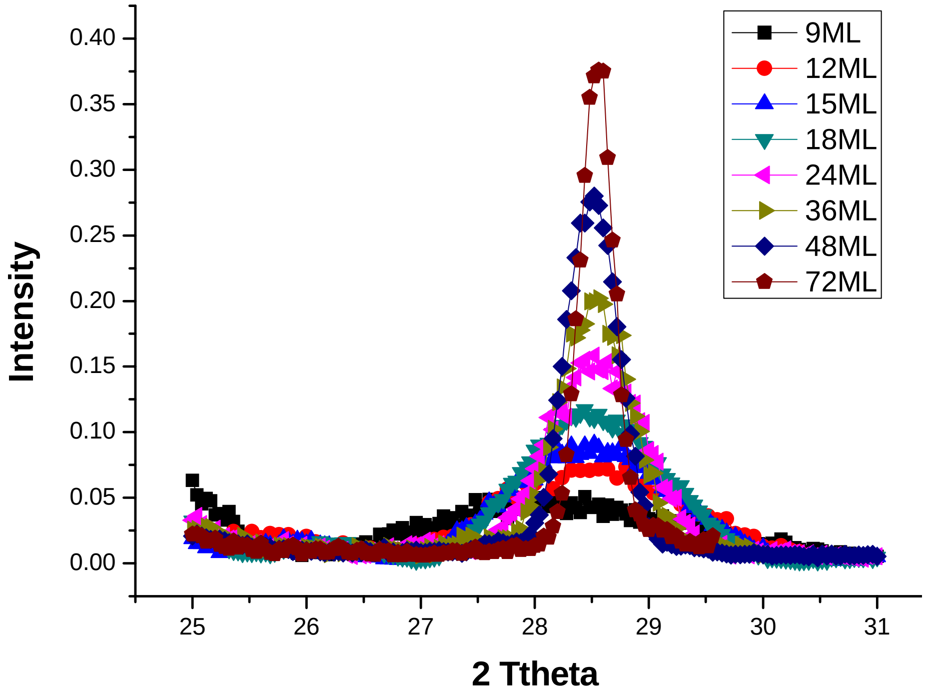

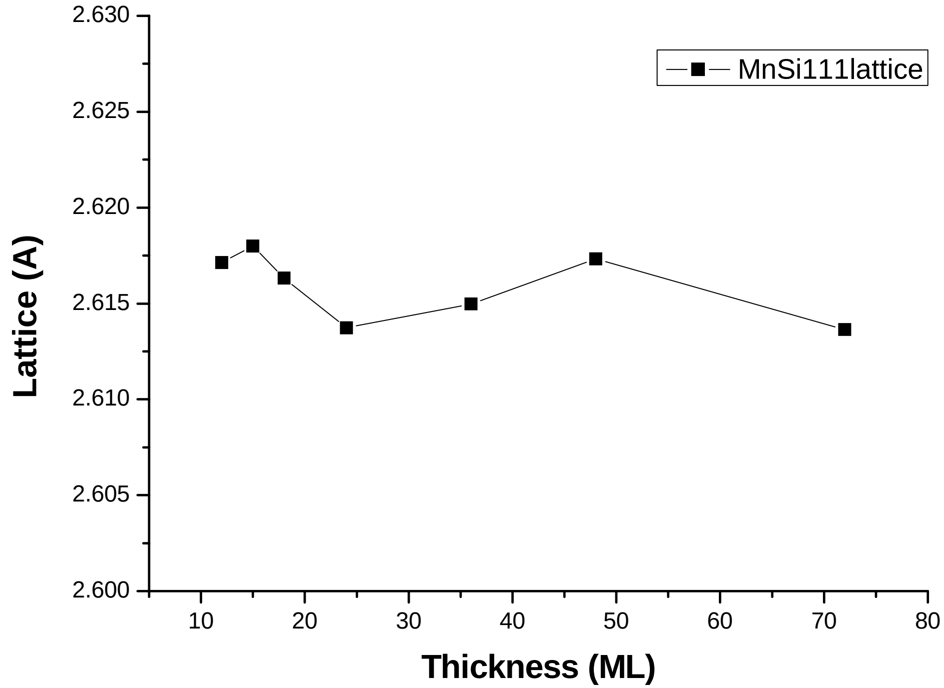

IV. Magnetic and Magnetotransport Properties of MnSi Ultrathin films

GMR Effect

24ML

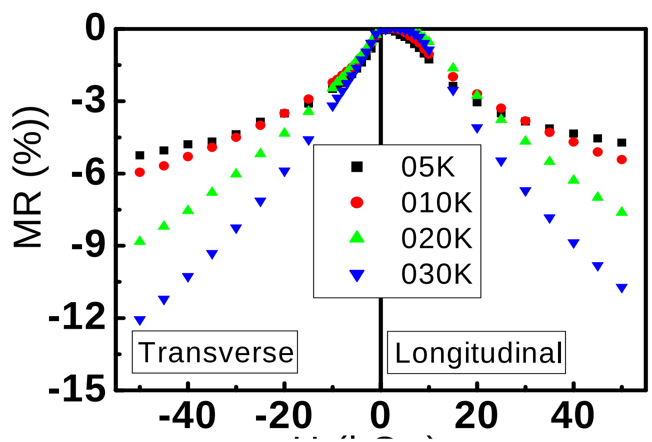

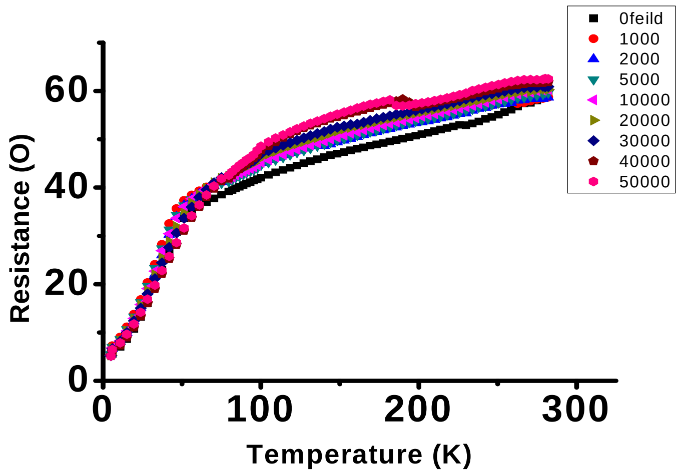

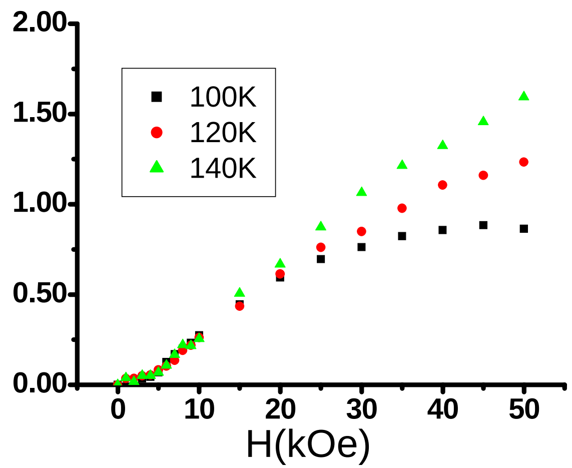

6 ML

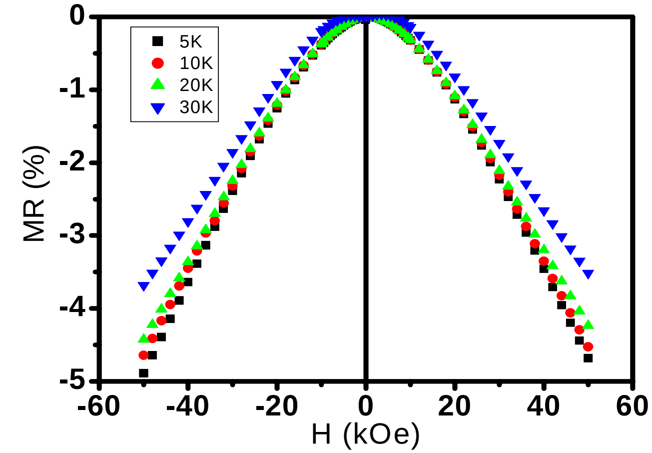

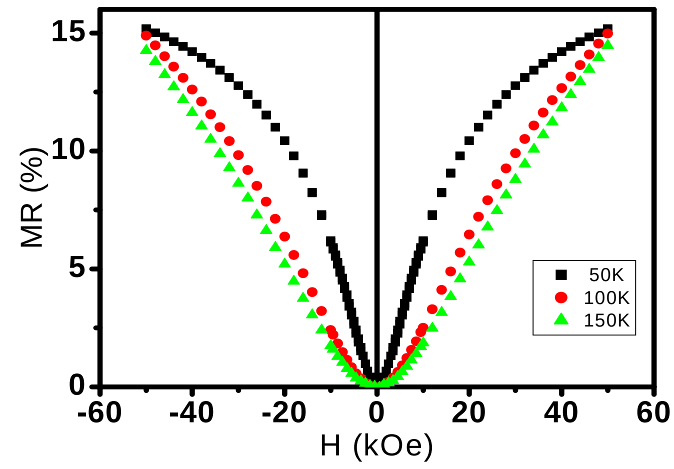

V. Thickness-driven MIT Transition of MnSi films

24ML

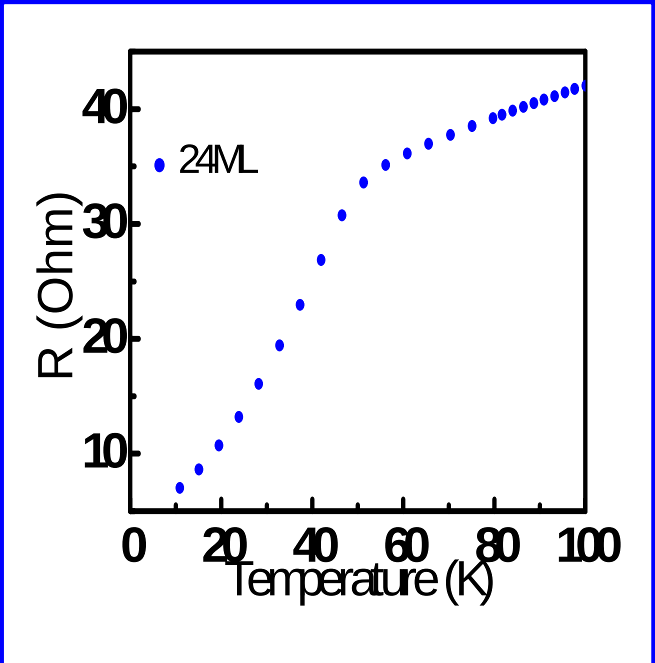

6ML

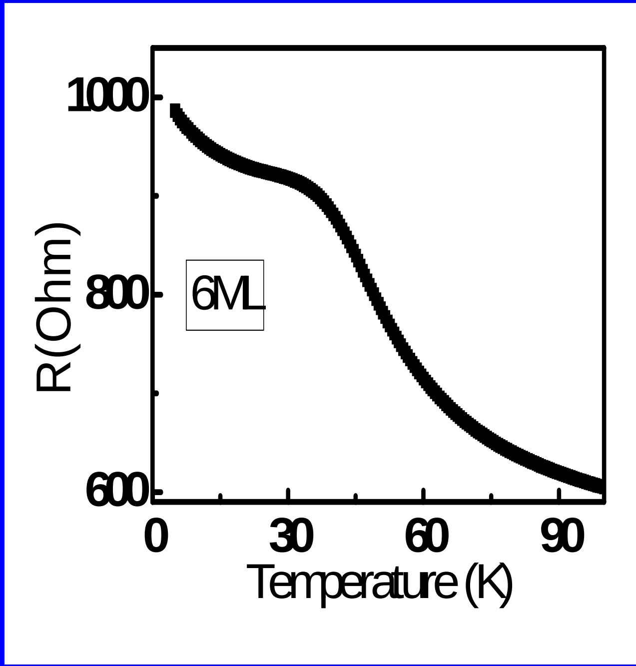

4ML

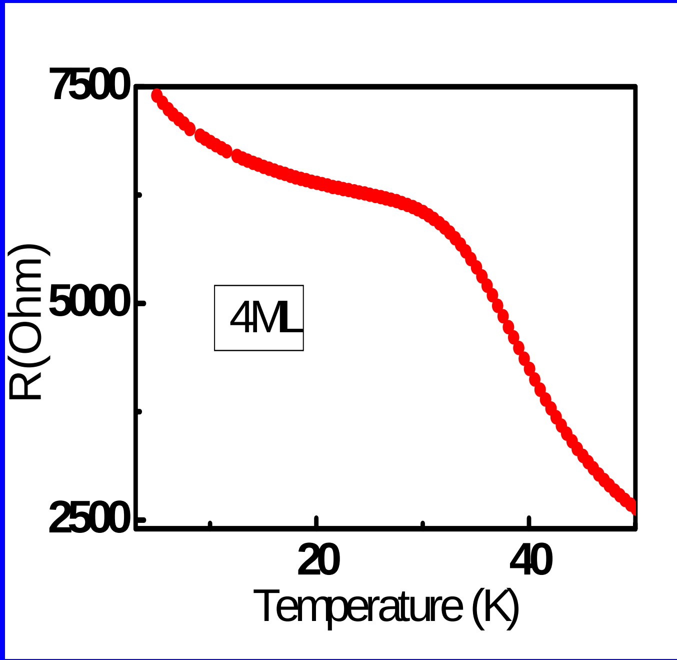

V. Thickness-driven MIT Transition of MnSi films

24ML **6ML** **4ML**

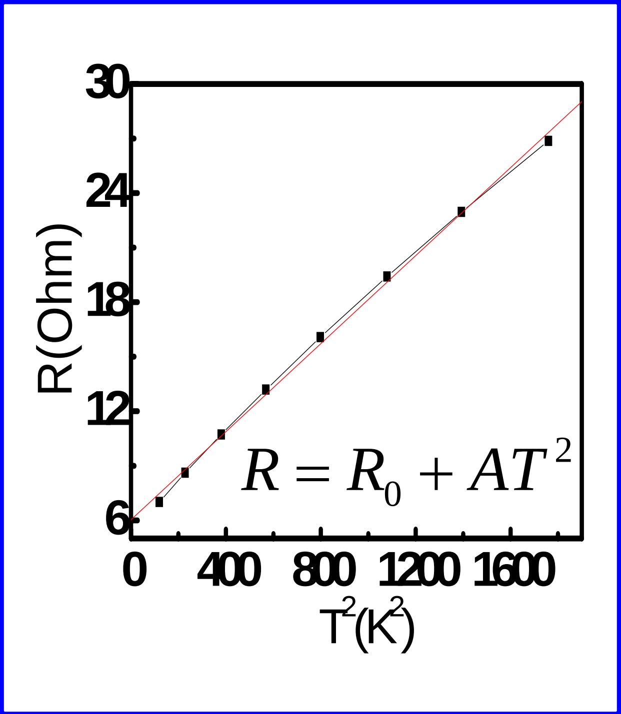

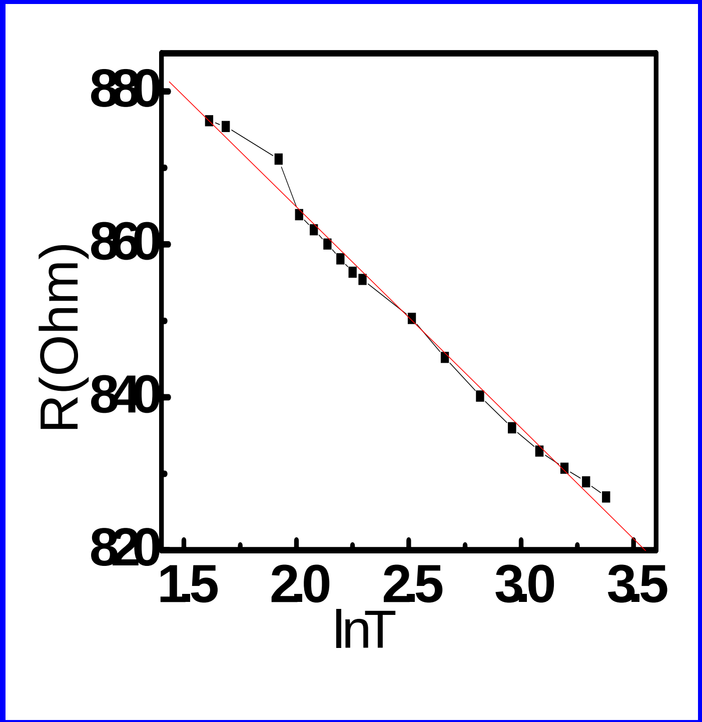

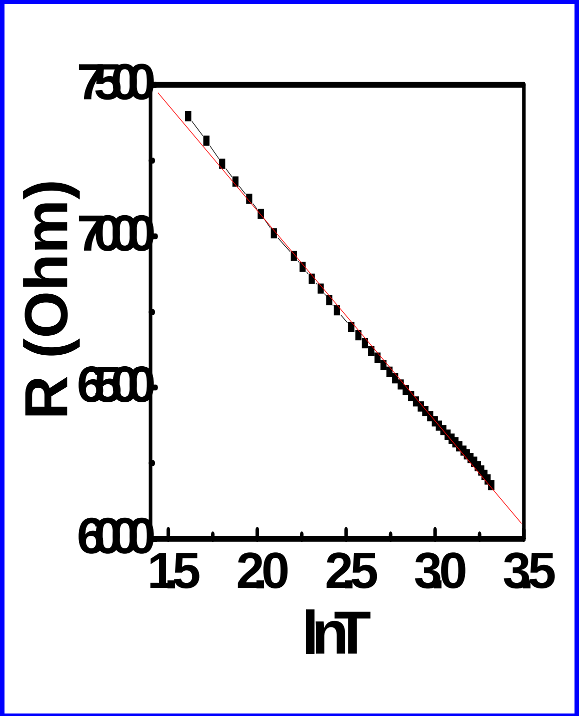

weakly itinerant electron ferromagnetic

2D system –weak localization

Resistivity decreases logarithmically with T

IV. Thickness-driven MIT Transition of MnSi films

Hall Effect

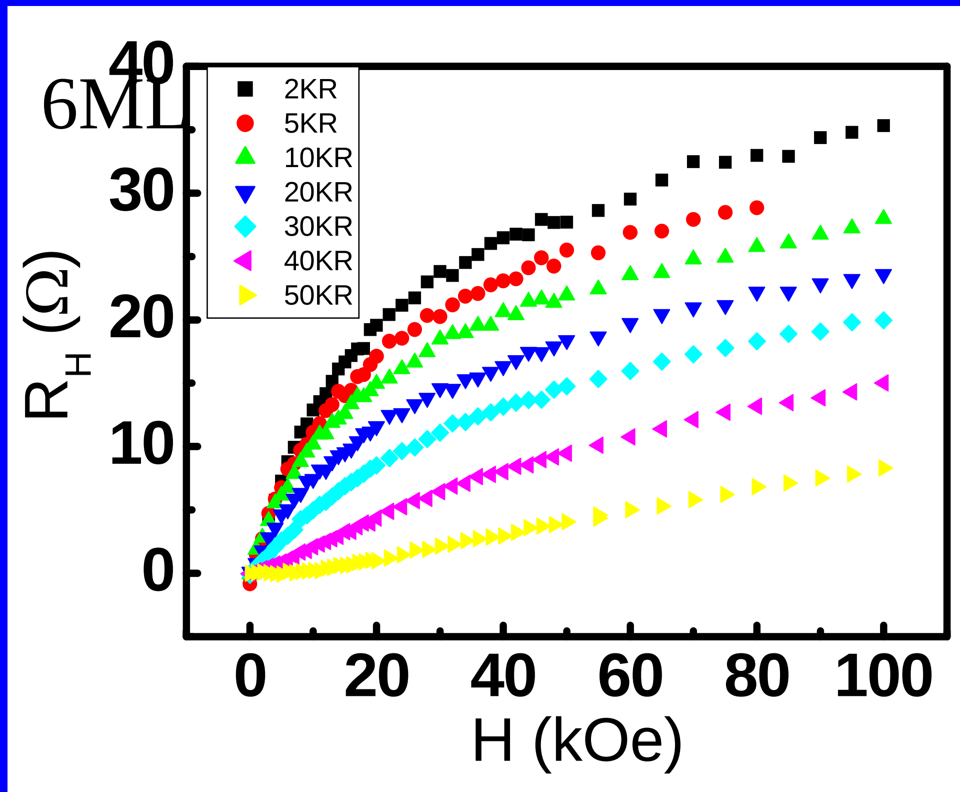

$$R_H = R_0 H + R_S M$$

VI. Summary and prospective

1. MnSi ultrathin film can be epitaxially grown on Si(111)-7×7 surface .
2. Thickness-driven Metal to Insulator Transition was observed in MnSi ultrathin film
3. Temperature dependence of resistivity indicates a weak localization 2D-system.
4. MnSi ultrathin film shows the advantages of both ferromagnet as well as semiconductor.
5. Investigation of morphology-dependent Magnetotransport provides a new idea for spintronics

Acknowledgements

- MOST
- NSFC
- CAS